

1-1-2016

## Strike-slip neotectonic regime and related structures in the Cappadocia region: a case study in the Salanda basin, Central Anatolia, Turkey

ALİ KOÇYİĞİT

UĞUR DOĞAN

Follow this and additional works at: <https://journals.tubitak.gov.tr/earth>



Part of the [Earth Sciences Commons](#)

---

### Recommended Citation

KOÇYİĞİT, ALİ and DOĞAN, UĞUR (2016) "Strike-slip neotectonic regime and related structures in the Cappadocia region: a case study in the Salanda basin, Central Anatolia, Turkey," *Turkish Journal of Earth Sciences*: Vol. 25: No. 5, Article 1. <https://doi.org/10.3906/yer-1512-9>  
Available at: <https://journals.tubitak.gov.tr/earth/vol25/iss5/1>

This Article is brought to you for free and open access by TÜBİTAK Academic Journals. It has been accepted for inclusion in Turkish Journal of Earth Sciences by an authorized editor of TÜBİTAK Academic Journals. For more information, please contact [academic.publications@tubitak.gov.tr](mailto:academic.publications@tubitak.gov.tr).

## Strike-slip neotectonic regime and related structures in the Cappadocia region: a case study in the Salanda basin, Central Anatolia, Turkey

Ali KOÇYİĞİT<sup>1</sup>, Uğur DOĞAN<sup>2,\*</sup>

<sup>1</sup>Department of Geological Engineering, Active Tectonics and Earthquake Research Laboratory, Middle East Technical University, Ankara, Turkey

<sup>2</sup>Department of Geography, Ankara University, Ankara, Turkey

Received: 14.12.2015 • Accepted/Published Online: 23.05.2016 • Final Version: 24.10.2016

**Abstract:** The study area is a strike-slip basin of approximately 1–9 km wide, 66 km long and N65°W trending, located between the historical Kesikköprü in the west and the Sarıhıdır settlement in the east along the northern side of the Central Anatolian Volcanic Province. It was evolved on a regional erosional surface of a pre-Quaternary volcanosedimentary sequence during Quaternary. This is evidenced by the stratigraphical, structural, and seismic data. The total amounts of throw and dextral strike-slip displacement accumulated on the basin-boundary faults during the evolutionary history of the basin are 178 m and 5 km, respectively. The average slip rate on the Salanda master fault is approximately 4 mm/year since the late early Pleistocene based on the total dextral strike-slip offset accumulated on it. The throw amount is small compared with the dextral strike-slip offset, which implies a strike-slip regime rather than a tensional tectonic regime in the basin. This is also supported by the combination of both the contractional and extensional structures such as reverse faults, fissure-ridge travertines, and a series of stepped terraces of late Quaternary age. Finally, it would be useful to take this paper into account in new works to be carried out in other sections of the Cappadocia region, because a new neotectonic regime (strike-slip tectonic regime) is first introduced here for this region.

**Key words:** Central Anatolian Volcanic Province, Cappadocia, Salanda basin, strike-slip neotectonic regime, Kızılırmak River, Quaternary

### 1. Introduction

In general, the neotectonic frame of Turkey and its near environs is determined by three major structures (Şengör and Yılmaz, 1981), namely the Anatolian platelet, its boundary faults (the dextral North Anatolian and the sinistral East Anatolian Fault Systems), and the southern Aegean-Cyprus subduction zone (Figure 1a). Currently, the southwestern section of the Anatolian Platelet is characterized by a tensional tectonic regime and related horst-graben systems, whereas its eastern part is under the influence of a strike-slip neotectonic regime and related structures such as dextral to sinistral strike-slip faults and pull-apart basins (Figure 1b). The effects of both the tensional tectonic regime and related structures run eastward up to the Salt Lake Fault Zone, which forms a transitional zone between the westerly located extensional and easterly located contractional neotectonic domains. One of the tectonomorphologically and historically fascinating areas in the Anatolian platelet is the Central Anatolian Volcanic Province (CAVP: the gray-shaded area

in Figure 1b) or Cappadocia, which etymologically means “the land of beautiful horses”. The CAVP is a 1.5-km-high volcanosedimentary plateau above sea level. It is about 15–90 km wide and 300 km long with a NE trending continental paleomagmatic arc (Keller, 1974; Pasquare et al., 1988) located in the area between Karaman in the southwest and Tuzla Lake in the northeast (Figure 1b).

A number of investigations of various purposes have been carried out in the CAVP. These deal mostly with the stratigraphy, tectonics, geomorphology, volcanology, petrology, and geochemistry of the CAVP and its geothermal potential. However, some significant controversial opinions among previous researchers are still under debate. They are mostly regarding the styles of the tectonic regime and the phases of volcanic activity accompanying them. Pasquare et al. (1988) suggested that the Middle Miocene-Quaternary volcanism in Central Anatolia is related to brittle deformation caused by the collision of the African-Arabian plates with the Eurasian plate and that the structural pattern of Central Anatolia is

\* Correspondence: [ugdogan@yahoo.com](mailto:ugdogan@yahoo.com)

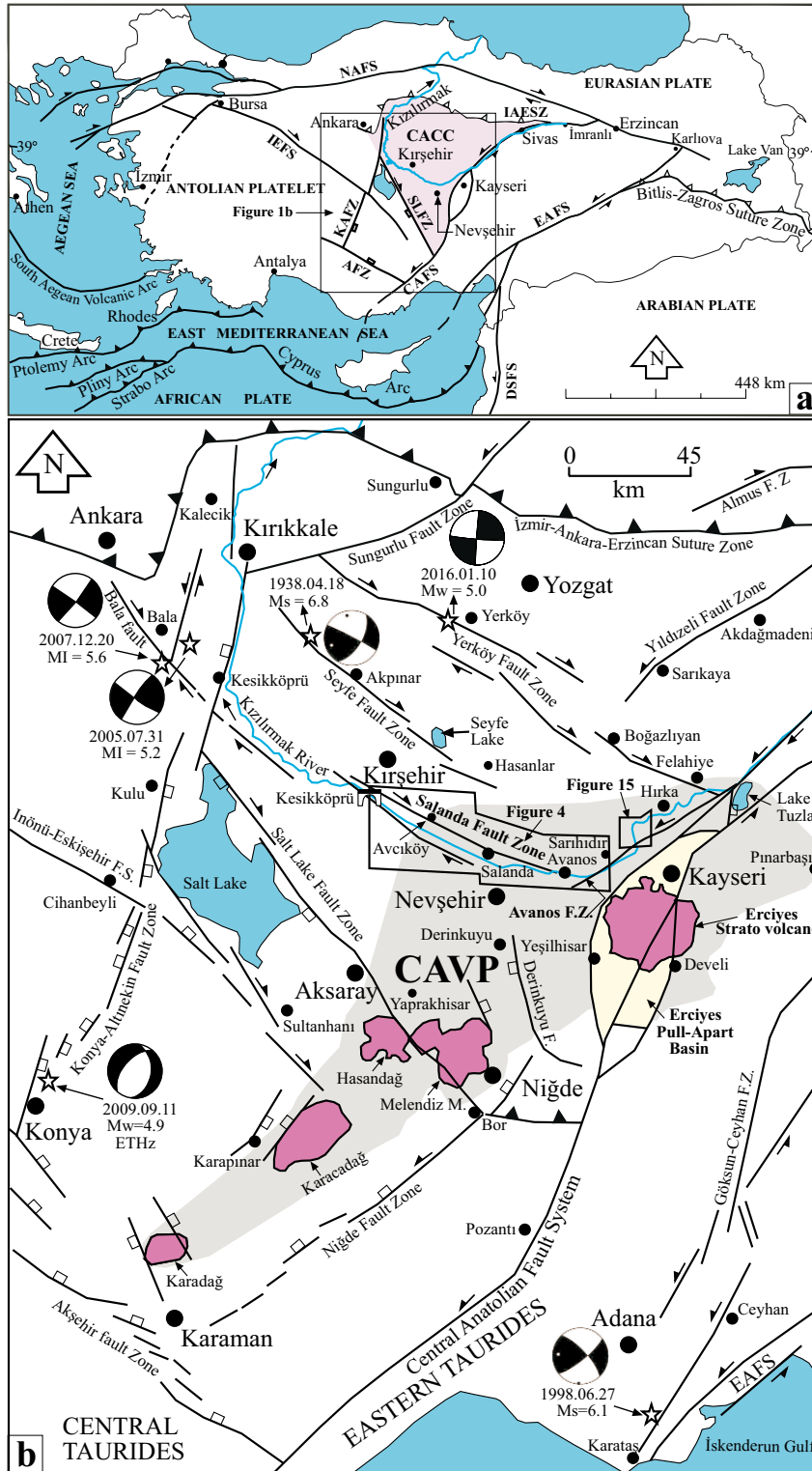


**Figure 1.** a) Simplified map showing both the plate tectonic configuration of Turkey and the site of the Central Anatolian Crystalline Complex (CACC: area in pinkish color). AFZ, Akşehir Fault Zone; CAFS, Central Anatolian Fault System; DSFS, Dead Sea Fault System; EAFS, East Anatolian Fault System; IEFS, İnönü-Eskişehir Fault System; IAESZ, Izmir-Ankara-Erzincan Suture Zone; SLFZ, Salt Lake Fault Zone; KAFZ, Konya-Altınekin Fault Zone; NAFS, North Anatolian Fault System. b) Simplified tectonic map showing the major structures, destructive earthquakes epicenters (stars), Central Anatolian Volcanic Province (CAVP: shaded area), and the site of the study area in and near the environs of the CACC (focal mechanism solutions are from Tan et al., 2008, 2010; USGS, 2016).

characterized mainly by three fault sets (the N320–340°, N-S, and N20–40° trending fault sets); they are connected with a stress field related to the N-S convergence between the African and Turkish plates, i.e. the nature of the prominent neotectonic regime in Central Anatolia is a strike-slip one. In contrast, Genç and Yürür (2010) suggested that the origin of the Middle Miocene-Quaternary volcanism in the CAVP is the asthenospheric upwelling related to a regional tensional tectonic regime and that the structural pattern of Central Anatolia is characterized by low-angle normal faults (e.g., “Kırşehir detachment fault”). Apart from these two regional works, there are also some other relatively local studies dealing with the stratigraphy and tectonics of the CAVP. Their ideas on the age and style of the tectonic regime, which affected the CAVP, can be categorized into two groups: 1) the tectonic regime in the CAVP is tensional in nature and continuous since late Miocene time (Toprak and Göncüoğlu, 1993; Toprak, 1994, 1996; Köksal and Göncüoğlu, 1997; Dhont et al., 1998; Dirik et al., 1999; Dirik, 2001, Özsayın et al., 2013), and 2) the CAVP has experienced an episodic evolutionary history during the late Middle Miocene-Quaternary, i.e. the tectonic regime is not continuous from the late Miocene to Recent. Both the episodic evolutionary history and the Quaternary strike-slip tectonic regime to related structures in the CAVP are first introduced to the literature in our study. This is the major difference between previous works and our study. This episodic evolution began and evolved under the control of a tensional tectonic regime during late Middle Miocene-late Pliocene time, but it was interrupted and replaced by a strike-slip neotectonic regime during early Quaternary time (2.588 Ma BP) (İnan, 1993; Koçyiğit and Beyhan, 1998; Koçyiğit and Erol, 2001; Ocakoğlu, 2004; Temiz, 2004). This new regime is here termed as a “strike-slip neotectonic regime” in the present paper. Thus, the present study aims to discuss this strike-slip neotectonic regime under the light of prominent dextral strike-slip offsets, very widespread fissure-ridge travertine occurrences, reverse faults, and the deposition of river terraces accompanied by the third phase of volcanic activity of Pasquare et al. (1988). One of the type localities dominated by these structures is the historical Kesikköprü-Sarıhıdır section of the Kızılırmak Valley. It also contains the Salanda basin and is located on the northern section of the CAVP (Figure 1b). Therefore, this region was chosen as the study area. It has not been mapped at 1/25,000 scale and studied in detail until the present study. Additionally, this study also aims to define the initial establishment and incision of the antecedent Kızılırmak River into its present-day position in the modern Salanda basin. We think that this new field work will produce an important contribution to the neotectonics of the Cappadocian region. The data used in this manuscript were collected

by usage of both office and field methods. These included the computer program T-TECTO 3.0, satellite images, aerial photograph and thin-section studies, detailed field geological mapping of rocks and faults at the scale of 1/25,000, and the measuring of both stratigraphical section and slip-plane data on fault slickensides. Aerial application of these methods was carried out in the framework of two major projects, 112Y153 and 07-03-09-1-00-23, supported by the Scientific and Technological Research Council of Turkey (TÜBİTAK) and Informatic Engineering (BM), respectively. Additionally, several short-term (1-week) field studies were also carried out with our own financial support in the period between 2008 and 2015. Therefore, this manuscript is an original paper, not an overview based on compiled information.

## 2. Regional geological setting

At a regional scale, the CAVP is located on two continental fragments (the Central Anatolian Crystalline Complex, CACC; and the Taurides) that rifted away from Gondwana probably during Triassic time (Şengör and Yılmaz, 1981; Frizon de Lamotte et al., 2011). Both continental fragments and the CAVP are crossed and divided into numerous blocks of dissimilar size by a series of active intraplate structures (Figure 1b). The present configuration of the CACC is approximately triangular in shape and bounded by three major structures, namely the Salt Lake Fault Zone in the west, the Central Anatolian Fault System in the east-southeast (Koçyiğit and Beyhan, 1998; Koçyiğit 2008), and the İzmir-Ankara-Erzincan suture zone in the north (Figure 1b). The latter resulted from the late Cretaceous-early Paleogene closure and the collision history of the northern strands of the Northern Neo-Tethys. It is characterized by a south-verging fold-imbricate thrust to reverse fault zone of colored ophiolitic mélangé (Koçyiğit, 1976; Şengör and Yılmaz, 1981; Seymen, 1984; Koçyiğit, 1991; Koçyiğit et al., 1995; Koçyiğit and Devci, 2008; Gülyüz et al., 2013). The Salt Lake Fault Zone was first recognized and named by Beekman (1966). It is 1–7 km wide and 170 km long with a NW-SE trending intraplate zone of active deformation in the nature of normal faulting with a considerable amount of strike-slip component. The normal fault character of the Salt Lake Fault Zone was identified once more by a recent detailed geological and paleoseismological study carried out on its central part (Kürçer et al., 2012). The Salt Lake Fault Zone begins from the Bor district in the southeast and then runs towards the northwest up to the northwestern tip of the Salt Lake, where it intersects with the NNE trending Konya-Altinekin oblique-slip normal fault zone and then terminates, i.e. it does not run further north-northwest (Figure 1b). Within this frame, the active fault segments (e.g., the Bala fault) around the Bala district do not comprise the continuation of the Salt

Lake Fault Zone due to the fact that they are strike-slip faults in nature as indicated by a series of recent seismic activities and their focal mechanism solution diagrams (Figure 1b). Consequently, the Bala fault segments form the northwestern continuation of the Salanda strike-slip fault zone, which is one of major structures of the present paper. The Salt Lake Fault Zone determines and controls the northeastern margin of the Salt Lake graben. One of the other significant intraplate structures is the Konya-Altınekin Fault Zone. It is 0.3–25 km wide, 270 km long, and a NNE trending active zone of deformation in the nature of oblique-slip normal faulting. The city of Konya is located in the southern section and the district of Kalecik is in the north of this fault zone, which intersects with several NW trending active fault zones such as the Akşehir, İnönü-Eskişehir, Salanda, and Sungurlu Fault Zones along its length (Figure 1b). The Konya-Altınekin Fault Zone consists of discontinuous, easterly- and westerly-dipping numerous stepped 2–32 km long normal fault segments with a maximum throw of 0.8 km.

The Central Anatolian Fault System is approximately 730 km long and 2–80 km wide, a NE trending very young neotectonic structure in the nature of sinistral strike-slip faulting (Koçyiğit and Beyhan, 1998; Koçyiğit and Erol, 2001). It resulted from the reactivation and propagation of an older paleotectonic structure, the so-called “Ecemiş corridor” (Blumenthal, 1941) or “Tekir Dislocation” (Metz 1956), in both the NNE and SW directions across the Inner Tauride Suture in early Quaternary time. One of the other intraplate strike-slip fault zones very close to the study area is the Seyfe Fault Zone. It is located between the town of Hasanlar in the southeast and Kırıkkale in the northwest (Figure 1b). It is 1–20 km wide, 165 km long, and a NW trending zone of active deformation in the nature of dextral strike-slip faulting. It consists of discontinuous numerous fault segments that are 1–30 km long. One of the destructive earthquakes ( $M_s = 6.8$ , 19 April 1938 Akpınar earthquake) that sourced from the Seyfe Fault Zone indicated once more its activeness (Figure 1b). Another significant intraplate active structure is the Yeniköy Fault Zone. It is about 1–15 km wide and 180 km long, a NW-trending dextral strike-slip zone of deformation located around Felahiye to the SE and near east of Kırıkkale to the NW. A very recent seismic event, the 10 January 2016 Hacıduraklı (Çiçekdağı-Kırşehir) earthquake of  $M_w = 5.0$  (USGS, 2016), sourced from the Yerköy Fault Zone and indicated that it is an active strike-slip structure (Figure 1b). As is seen from the major structures and earthquake focal mechanism solution diagrams in Figure 1b, there is a prominent and active strike-slip structural pattern rather than a tensional tectonic regime in eastern Central Anatolia. The faults forming this structural pattern are linked to each other by a stress system, in which the

major principal compressive stress ( $\sigma_1$ ) is operating in an approximately N-S direction (Pasquare et al., 1988; Tan et al., 2008, 2010).

The CACC consists of five rock assemblages (Figure 2). These are, from oldest to youngest: 1) Paleozoic to Mesozoic metamorphic rocks (Kırşehir, Niğde, and Akdağ massifs), 2) Upper Cretaceous colored ophiolitic mélangé (Anatolian Nappe), 3) granitoidic to syenitoid intrusions of late Maastrichtian-early Paleocene age (Akçataş Granitoid), 4) volcanic series (Kızıltepe Volcanics) of late Maastrichtian-early Paleocene age, and 5) Paleogene and Quaternary marine to continental cover sequences (Erkan, 1981; Seymen, 1984; Aydın, 1991; Tolluoğlu, 1993; Köksal and Göncüoğlu, 1997; Whitney et al., 2001; Gautier et al., 2002; Kadioğlu et al., 2006; Gautier et al., 2008; Koçyiğit and Devci, 2008; Boztuğ et al., 2009; Genç and Yürür, 2010; Gülyüz et al., 2013). They are separated from each other by intervening long- to short-term erosional periods (unconformities and diastems, respectively) and tectonic contacts, i.e. low-high angle reverse faults (Figure 2). The pre-Quaternary rocks are here termed as paleotectonic units. The most diagnostic and youngest paleotectonic unit is the Ürgüp group of late Middle Miocene-Pliocene age. In order to make a distinction between the paleotectonic and neotectonic periods, both the Ürgüp group and the modern basin fill (Quaternary Salanda group) will be described in detail below.

### 3. Basin fills

#### 3.1. Ürgüp group

It was first recognized and introduced to the literature as the “Ürgüp Formation” by Pasquare (1968). However, it was shifted to the rank of group in the present paper owing to the fact that it contains several lithofacies that can be mapped at 1/25,000 scale. In general, the Ürgüp group is over 1 km thick but it decreases up to several tens of meters towards the north of the study area. It is tilted to open folded and overlain with a regional angular unconformity by the nondeformed (nearly flat-lying) Salanda basin fill of Quaternary age (the Salanda group) (Figures 2 and 3). The Ürgüp group consists mostly of lavas of dissimilar composition, ignimbrites, and other pyroclastic rocks alternating with the fluviolacustrine sedimentary facies. The oldest volcanic rock included in the Ürgüp group is of the Middle Miocene (13.7–12.4 Ma) and is located across the Keçikalesi and Kızılcın volcanoes outside the study area (Besang et al., 1977; Batum, 1978). The Ürgüp group is an older and more widespread fill located in and outside of the Salanda basin (Figures 3 and 4). It was deposited under the control of a tensional tectonic regime over a broad area including the earlier site of the recent Salanda strike-slip basin. The bottom of the Ürgüp group is found near the west of the Tuzköy settlement

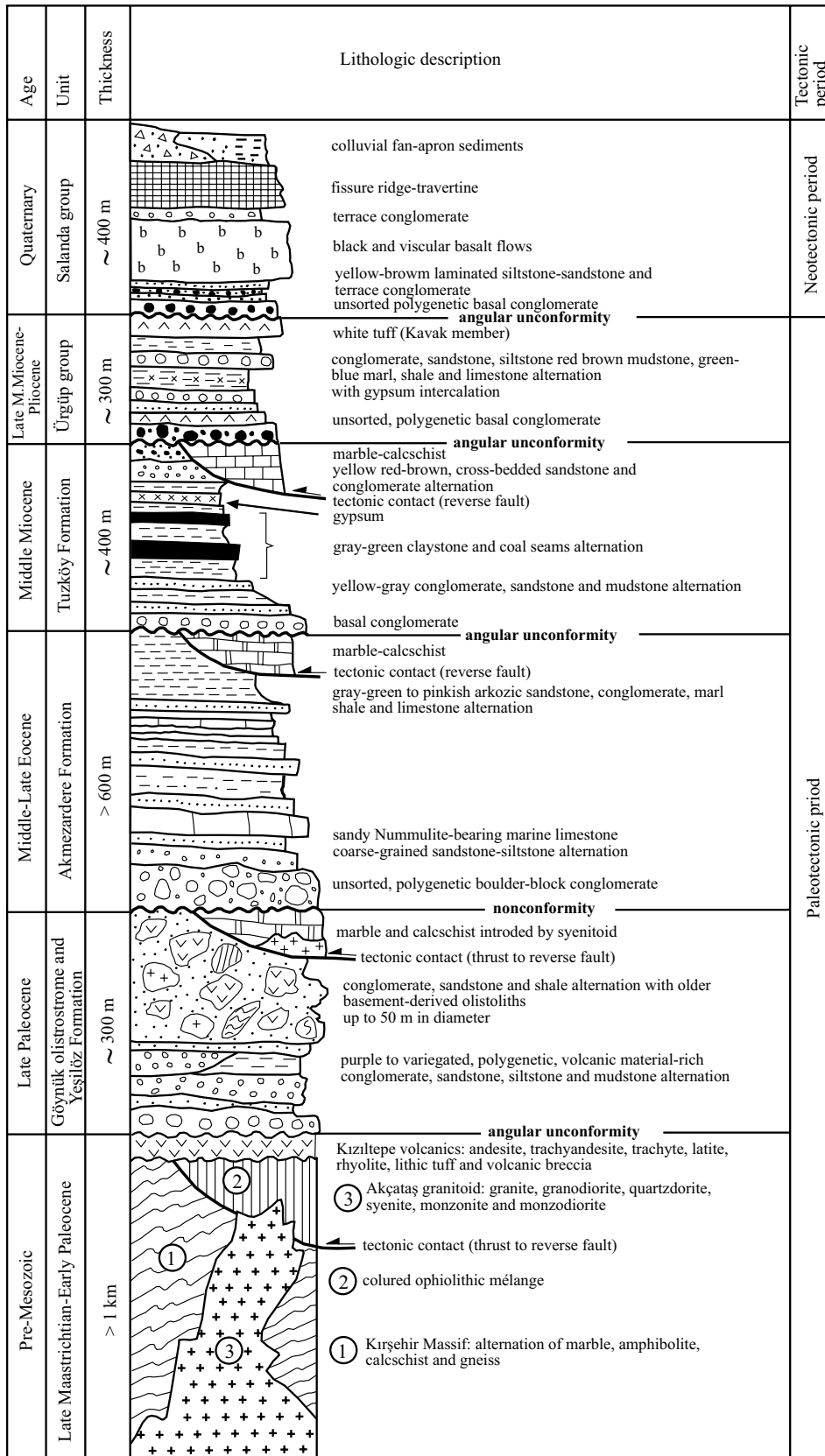


Figure 2. Simplified and combined tectonostratigraphic column showing basement and cover sequences forming the CACC.

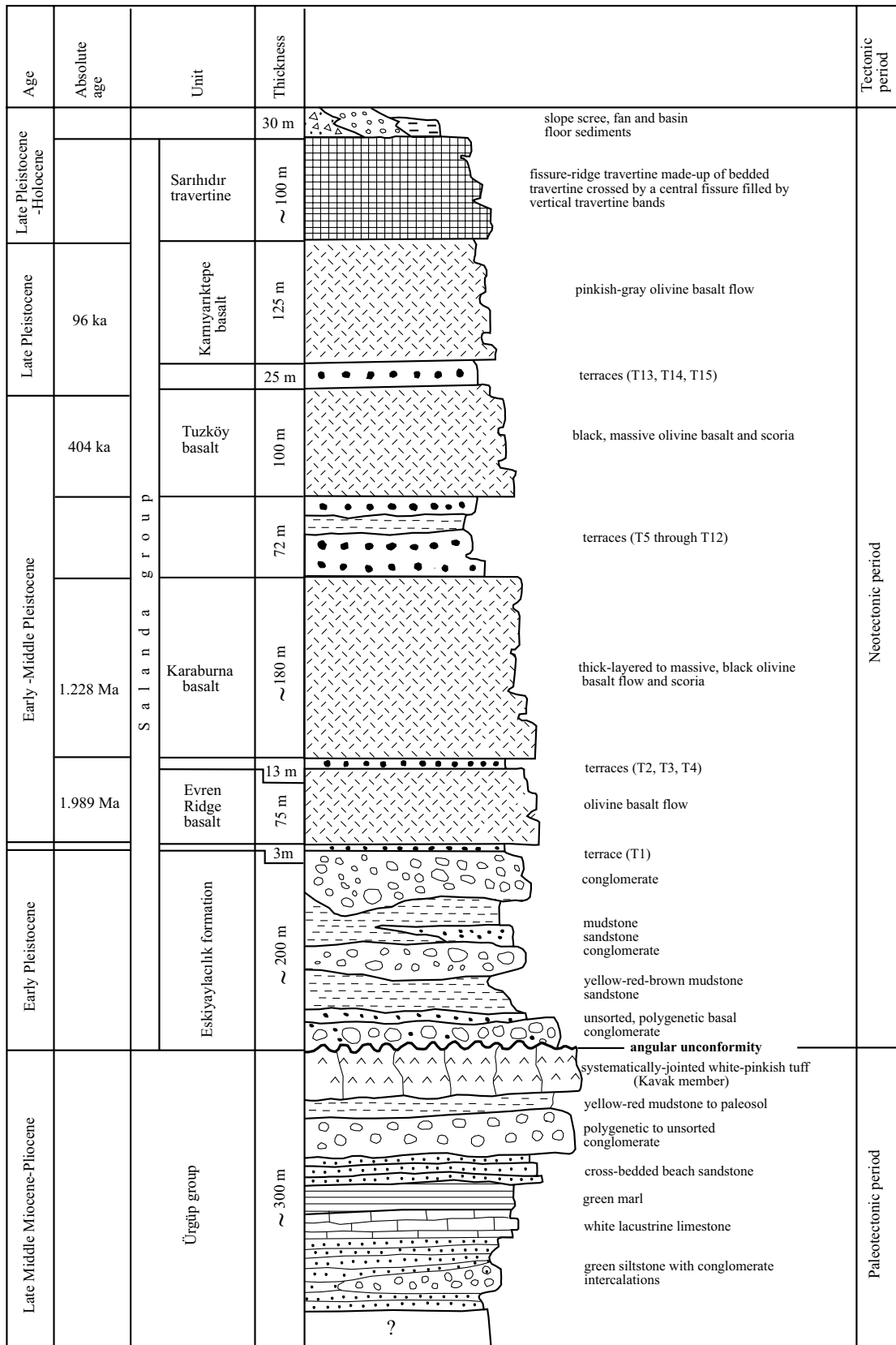


Figure 3. Simplified stratigraphical column of the Salanda strike-slip basin.





along the southern margin of the Salanda basin. At this locality the gray-yellow and gently dipping colored fluvial clastic rocks (basal conglomerate, sandstone, siltstone, mudstone alternation) of the Ürgüp group superimpose with an angular unconformity the steeply tilted to folded yellow-red conglomerate, sandstone, shale, and gypsum alternation of the Middle Miocene Tuzköy Formation (Akgün et al., 1995). These basal clastics of the Ürgüp group are succeeded by the alternation of pumice clast-bearing pinkish tuff-ignimbrite, white and well-bedded tuff, pyroclastics in the nature of lahar deposits, white and thin-bedded to laminated limestone, and medium-bedded to porous lacustrine limestone at the topmost. Lastly they are overlain with an angular unconformity by Quaternary basalt flows such as the Evren Ridge and Tuzköy and Karnıyarıktepe basalts in the Gülşehir-Tuzköy area (Figure 3). However, in the further south-southeast and outside the study area (along the west-northwest margin of the Erciyes pull-apart basin), the resting facies, forming the uppermost part of the Ürgüp group, are still exposed (Koçyiğit and Beyhan, 1998). In that area, the Ürgüp group ends with a key horizon, the Valibabatepe Ignimbrite, whose Ar/Ar and K/Ar ages range between 2.52 and 3.0 Ma (Pasquare, 1968; Innocenti et al., 1975; Koçyiğit and Erol, 2001; Le Pennec et al., 2005; Aydar et al., 2012). This key horizon conformably overlies the lacustrine Kışladağ limestone, which is the second lithofacies from the top of the Ürgüp group. These regional field observations reveal that the topmost part of the Ürgüp group accumulated in the northern areas might have been eroded before the development of the Salanda strike-slip basin. This is also supported by the observations made inside the basin. These are: 1) the bottom of the Ürgüp group is not seen inside the Salanda basin, and 2) the upper half of the Ürgüp group is absent in the Salanda basin while it is exposed in the south-southeast and outside the Salanda basin. However, its observable lowermost part begins with the green-colored to thin-bedded siltstone beds with polygenetic conglomerate intercalations and then continues upward with the alternation of white lacustrine limestone, green to blue marl-shale, polygenetic to unsorted conglomerate with sandstone intercalations, and yellow-red mudstone. This package of the Ürgüp group is full of synsedimentary features such as the normal type of growth faults and slump structures. The total thickness of this sedimentary package is 280 m. At the topmost, this sedimentary sequence is capped conformably by white-pinkish and systematically jointed ignimbrite that is 5–20 m thick (the Kavak member of Pasquare, 1968) (Figure 3). The upper and lower parts of this ignimbritic key horizon consist of white pumice beds made up of subrounded to angular pumice clasts up to 10 cm in size. The K-Ar age of the Kavak member is  $9.0 \pm 0.4$  Ma (Viereck-Goette et al., 2010). The ignimbritic

key horizon is overlain with an angular unconformity by the lowermost unit (the Eskiaylacık formation) of the Salanda group (Figure 5a).

### 3.2. Salanda group

This is the second and youngest volcanosedimentary sequence accumulated under the control of the strike-slip neotectonic regime. It consists of, from bottom to top, fluvial clastics (the Eskiaylacık formation), four basalt flows (Evren Ridge, Karaburna, Tuzköy, and Karnıyarıktepe basalt flows) separated by the intervening 15 terrace deposits of different thickness, the actively growing fissure-ridge travertines, and Holocene alluvial sediments (Figure 3).

#### 3.2.1. Eskiaylacık formation

It begins with a basal conglomerate on the erosional surface of the Kavak Ignimbrite of late Miocene age at the bottom (Figure 5a) and then is succeeded by the alternation of conglomeratic sandstone to sandstone, yellow-red-brown mudstone, and again conglomerate horizons. Lastly it is overlain conformably by a terrace deposit (Figure 3). Towards the top, clastics become loose and reach up to a total thickness of 200 m. Basal conglomerate of the Eskiaylacık formation is very hard, unsorted, and polygenetic in composition. It also contains planar cross-bedded lenticular sandstone intercalations in some places. Conglomerates consist of angular, subrounded to rounded pebbles to boulders (up to 40 cm in diameter) of marble, granite, syenite, schist, quartz, quartzite, andesite, basalt, diabase, chert, radiolarite, gabbro, peridotite, and serpentinite set in a volcanic material-rich sandy matrix bounded by iron and calcite cements. Very close to the bottom contact, the basal conglomerate also contains angular pumice clasts (up to 10 cm in size) derived directly from the underlying Kavak Ignimbrite of about 9 Ma old, which entails the long-term stratigraphical gap between the underlying Ürgüp group and the lowermost unit of the modern Salanda basin developed on it (Figure 5b). In addition, the Eskiaylacık formation is overlain conformably by the Evren Ridge basalt flow of 1.989 Ma old near the south of Tuzköy town along the southern margin and by the Karaburna basalt flow of 1.228 Ma old around Karaburna village along the northern margin of the Salanda basin, respectively. Based on these contact relationships, the Eskiaylacık formation is thought to be at least early Quaternary in age. In contrast, this unit has been previously reported as a lithofacies included in the older Ürgüp group (Toprak, 1994).

#### 3.2.2. Terrace deposits

Terrace deposits form the second and very significant unit of the Salanda group (Figure 3). Fifteen terrace horizons of different thicknesses and elevations, which range from 160 m to 5 m above the recent elevation of the Kızılırmak River bed, were identified and labeled as T1 through T15

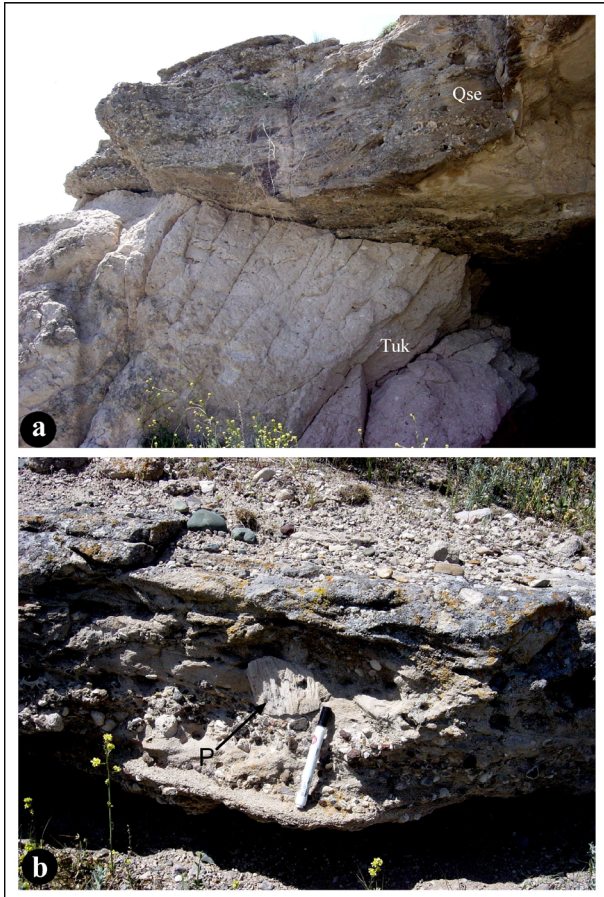


**Figure 5.** a) Close-up view of systematically jointed Kavak ignimbrite (Tuk) and the overlying basal conglomerate of the Eskiaylacık formation (Qse) (near NE of Yüksekli village). b) Close-up view of the pumice (P) clast-bearing basal conglomerate of the Eskiaylacık formation (NE of Yüksekli village).

by Doğan (2011) (Figure 6). They have not been plotted on the geological map (Figure 4) in order to avoid complexities (for more detailed information, readers are invited to refer to Doğan, 2011). Instead, a generalized cross-section (Figure 6) of the Kızılırmak Valley is provided. It shows the development order of terraces and their contacts and age relationships with the basalt flows. As is seen clearly from the cross-section, most of the terraces are located on the northern side of the river valley and unpaired in character, which implies the asymmetrical development history of the Salanda basin. By using terrace sequences and basalt ages, the time-averaged incision rate of the Kızılırmak river during the last 2 million years was determined as approximately  $\sim 0.08$  mm/year, but important variation within that time span is also apparent. The highest incision rate during this period was determined to be  $\sim 0.12$  mm/year between the late-early and mid-middle Pleistocene (Doğan, 2011).

### 3.2.3. Basalt flows

Basalt flows constitute the third unit of the Salanda group (Figures 3 and 4). Four basalt flows of dissimilar age and thickness were identified, mapped, named, and dated separately (Doğan, 2011). These are, from oldest to youngest, the Evren Ridge basalt ( $\beta_1$ :  $1989.4 \pm 38.9$  ka), the Karaburna basalt ( $\beta_2$ :  $1228.2 \pm 46.4$  ka), the Tuzköy basalt ( $\beta_3$ :  $403.8 \pm 9.8$  ka), and the Karnıyarıktepe basalt ( $\beta_4$ :  $96.0 \pm 13$  ka). They were crosscut and displaced in both horizontal and vertical directions by the margin-boundary master faults, namely the Salanda and Tuzköy faults (Figures 4 and 6). The Karaburna basalt is located around the Karaburç and Karaburna settlements along the northwestern margin of the Salanda basin while the other three basalt flows are found in the Gülşehir-Tuzköy area along the southern margin of the basin. The Gülşehir-Tuzköy Quaternary basalt flows were first studied and introduced into literature by Sassano (1964). He reported that they had been poured out of the Nevşehir-Acıgöl volcanic center (particularly from both the Karnıyarık and Susamsivrisi volcanoes, approximately 7–15 km south and outside the Salanda basin) and then flowed north-northwestward in a downslope direction. The Evren Ridge and the Karaburna basalts are reddish to black in color. Their lower parts are vesicular while the upper parts are massive and crossed by vertical to subvertical cooling cracks. Based on thin-section studies, both basalt flows are in the nature of olivine basalt and composed mostly of olivine phenocrysts set in a groundmass made up of augite, plagioclase, and volcanic glass. Even if the Evren Ridge and Karaburna basalt flows are more or less the same in mineralogical composition, they are not similar in terms of age and location (Figures 4 and 6). At present, the bottom of the Evren Ridge basalt flow is located on terrace T1 along the southern margin while the Karaburna basalt flow is located on terraces T2 and T4 along the northern margin (Figures 6 and 7) at elevations of 160 m and 138 m to 128 m, respectively, above the present-day Kızılırmak River bed (Figures 4 and 6). There was a deep depression (Salanda basin) drained by the Kızılırmak River between the southerly-located Evren Ridge basalt flow and the northerly-located Karaburna basalt flow during the early evolutionary stage of the Salanda basin. These observations satisfactorily reveal that the Karaburna basalt flow arrived to its present-day location during the middle stage of the Salanda basin development.

The Tuzköy and Karnıyarıktepe basalt flows are located on terraces T12 and T15 at elevations of 29 m and 5 m, respectively, above the present-day Kızılırmak River bed along the southern margin of the Salanda basin (Figures 4 and 6). They are dark gray to black in color, highly vesicular, and have a lobate structure. They are augite basalt in composition and made up mostly of pyroxene

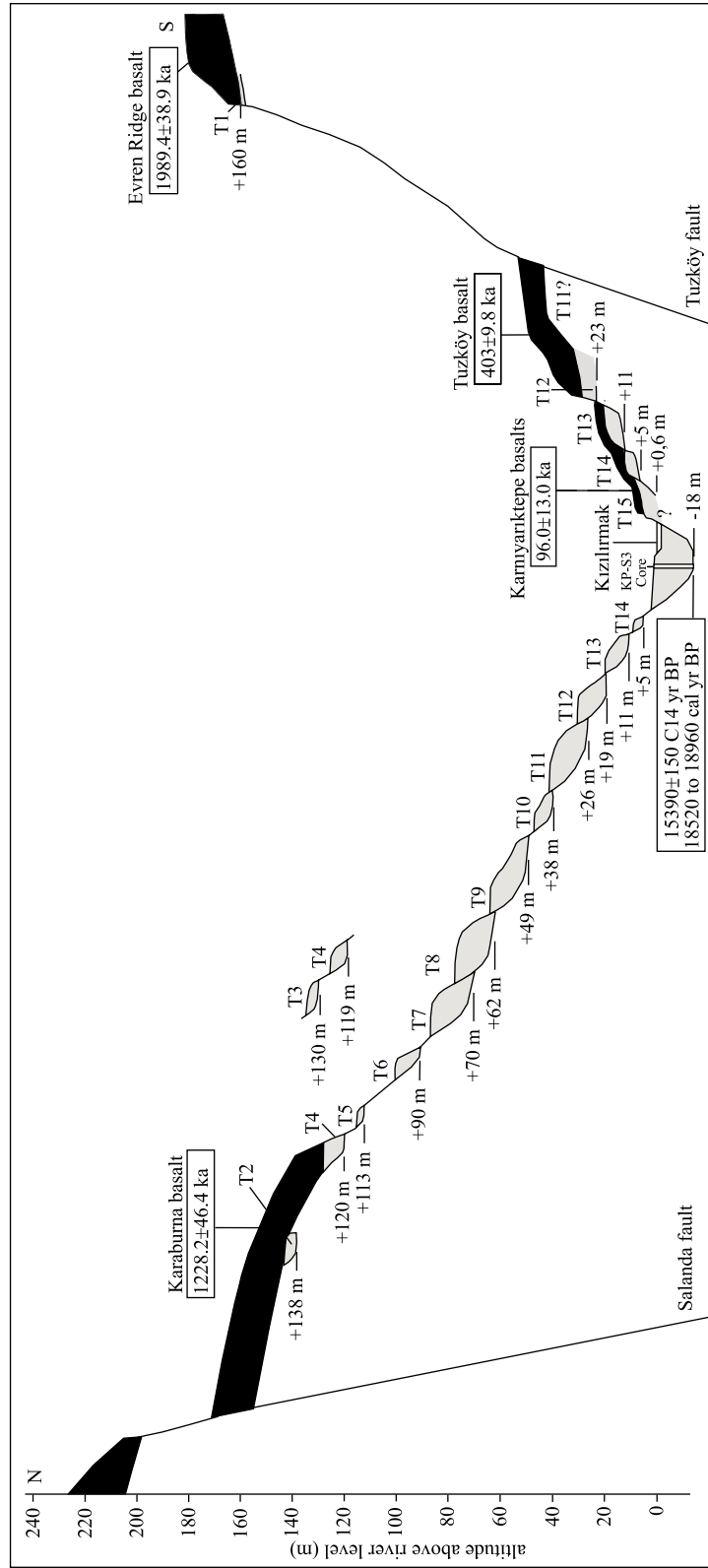


**Figure 6.** Sketched cross-section of the Kızılırmak River Valley in the Salanda strike-slip basin. It shows stepped pattern of 15 terraces developed at different elevations with respect to the current river bed and their relationships with the fissure ridge basalt flows (modified partly from Doğan, 2011).

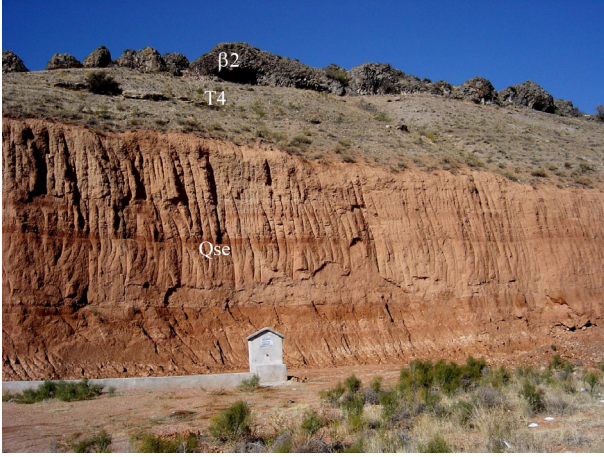


**Figure 7.** General view of Terrace 4 (T4) and the overlying Karaburna fissure ridge basalt flows of 1.228 Ma old ( $\beta_2$ ) (near the SSW of Karaburna village).

(augite) and plagioclase (oligoclase) phenocrysts set in a groundmass composed of very small-sized labradorite, andesine, and volcanic glass (Güleç, 1996). Both basalt flows were crosscut and displaced in vertical and lateral directions by the Tuzköy and Gülşehir faults (Figure 4).

#### 3.2.4. Travertines

The fourth and most significant unit of the Salanda group comprises the fissure-ridge travertine occurrences. In general, travertines are being deposited by calcium- and bicarbonate-rich cold to hot waters coming up and pouring out of the earth along the fractures. Active faults are the most suitable paths for the circulation of ground waters. At relatively deeper parts of the ground, the  $\text{CO}_2$  content of the ground water is considerably high, and it makes the water oversaturated in  $\text{CO}_2$  and thus inhibits both the precipitation of  $\text{CaCO}_3$  and formation of travertine. In contrast to this, both the  $\text{CO}_2$  and pressure suddenly release and make the water unsaturated in  $\text{CO}_2$  when they reach the ground surface, and thus formation of travertine is initiated. From this point of view, there is a close relationship between active faults and travertine occurrences. Travertines have been taken into account to be one of the significant recorders of the neotectonic activity throughout the last two decades (Altunel and Hancock, 1993; Altunel, 1996; Hancock et al., 1999; Koçyiğit, 2003, 2005; Temiz, 2004; Altunel and Karabacak, 2005; Brogi et al., 2005; Karabacak, 2007; Mesci et al., 2008). Hancock et al. (1999) reported the significance of travertine deposits in the recent tectonic development of a region and then proposed the term “travitonics” to emphasize the close relationship between the travertine formation and active tectonics. There is also a kinematic relationship between the general trend of the long central axis of the fissure-

ridge travertine and the operation direction of the major principal stress ( $\sigma_1$ ), which controlled the development of fissure-ridge travertine. In the case of a strike-slip tectonic regime, the central long axis of the fissure-ridge travertine is more or less parallel to the operation direction of  $\sigma_1$ , but it is perpendicular to the operation direction of  $\sigma_1$  in the case of tensional tectonic regime and related normal faulting. The study area and the nearby environment are the type localities for the widespread fissure-ridge travertine occurrences. However, except for the Kırşehir travertines exposed in the north and outside the study area, they have not been studied and documented until now. Fissure-ridge travertines are well developed and exposed on both the northern and southern fault-bounded margins of the Salanda basin (Figure 4). These are, from west to east, the Kızıltepe (Avcıköy), the Salanda (Gümüşkent), the Balkaya-Boztepe (Avanos), and the Sarıhıdır and the Karadağ fissure-ridge travertines (Stations 1, 2, 3, 4, and 5 in Figure 4). The general characteristics of these travertines are more or less same. Therefore, only two of them (the Kızıltepe and Sarıhıdır travertines) will be described in detail below.

The Kızıltepe travertines are exposed in a 1-km-wide and 1.5-km-long zone around Kızıltepe between Avcıköy village in the north and Kızılağıl village in the south-southwest along the northwestern section of the Salanda Fault Zone (1 in Figure 4). At this locality two groups of travertines occur: 1) thick-bedded to massive, highly porous, gently dipping, and relatively older bedded travertines, and 2) long, curvilinear, and actively growing fissure-ridge travertines. Bedded travertine overlies with an angular unconformity the Lutetian Akmezardere Formation. However, the bottom of the fissure-ridge travertines is not observed. They display a structural pattern similar to a doubly plunging anticline with a curvilinear long central axis, which connects a series of spring orifices (Figure 8a). The general trend of the long central axis of the Kızıltepe fissure-ridge travertine ranges between  $\text{N}10^\circ\text{E}$  and  $\text{N}20^\circ\text{E}$ , i.e. it trends in the NNE direction and indicates the operation direction of the major principal stress ( $\sigma_1$ ) prevailing in the study area.

The Sarıhıdır travertines occur in an ENE trending zone of approximately 0.3–1 km wide and 6.5 km long in the north of Sarıhıdır Village (4 in Figures 4 and 8b). They conformably overlie the Eskiaylacık formation. However, the Sarıhıdır travertines are tectonically juxtaposed with both the Ürgüp group in the south and the Akçataş syenitoid in the north by fault segments of the Avanos Fault Zone (Figure 4). The Sarıhıdır travertines consist of two major types: 1) medium- to thick-bedded, gently dipping, and relatively older bedded travertines, and 2) actively growing fissure-ridge travertine with a structural pattern like a long, narrow, and doubly plunging anticline



**Figure 8.** a) Close-up view of the Kızıltepe (Avcıköy) fissure-ridge travertine (FR). The long central axis trends in the NNE direction and runs parallel to the operation direction of major principal compressive stress ( $\sigma_1$ ). b) General view of the Sarıhıdır travertines (FR) and its margin-boundary faults. BF, Bozca fault; SF, Sarıhıdır fault (view to the north). c) Close-up view of the Sarıhıdır fissure-ridge travertine (FR).

with steeply dipping and faulted limbs (Figure 8c). The opening amount of central fissure ranges from several centimeters to 40 cm. It is also normal faulted. The general trend of the long central axis of the fissure-ridge travertine ranges between N15°E and N30°E, i.e. it again trends in the NNE direction and indicates the operation direction of the major principal stress ( $\sigma_1$ ) controlling the development of the Sarıhıdır fissure-ridge travertine.

The travertine deposits in the study area have not been dated radiometrically. However, they must be late Pleistocene to Holocene in age based on the stratigraphical relationships among the travertine occurrences, Quaternary basalt flows, and terrace deposits in the Salanda basin (Figure 3). In addition, the fissure-ridge

travertines in the Salanda basin can be correlated with both the Yaprakhisar (Aksaray) and the Kırşehir fissure-ridge travertine occurrences (Figure 1b) based on their occurrence pattern and general trend of the long central axes and activity (Temiz, 2004; Karabacak, 2007; Temiz et al., 2009). The nearest and well-developed travertine occurrences are exposed at the city center of Kırşehir approximately 20 km northwest but outside the Salanda basin. The Kırşehir travertines (the Kayabaşı and the Kuşdili fissure-ridge travertines) were studied in detail and dated by using the U-series method. Based on this dating, the Kayabaşı and the Kuşdili travertines are 70145–96080 years (late Pleistocene) and 18040–8700 years old (late Pleistocene-Holocene), respectively (Temiz, 2004; Temiz

et al., 2009). These authors also reported that the long central axes of these fissure-ridge travertine occurrences range from N-S to N30°E in trend, i.e. they also trend in the NNE direction. As is seen clearly from these data, both the Kızıltepe and Sarlıdır fissure-ridge travertines fit well with both the Kayabaşı and Kuşdili fissure-ridge travertines in age and general trends of long central axes of fissure-ridge travertines. It can be concluded that the operation direction of the major principal stress ( $\sigma_1$ ) governing the strike-slip neotectonic regime is NNE. This implies that both Kırşehir and our study area altogether are under the control of the same tectonic regime and a compressive stress system. The operation direction (NNE) of  $\sigma_1$  obtained from the kinematic relationship between the strike-slip active tectonics and the general trend of long central axes of the fissure-ridge travertines is also proved by the operation direction (approximately N-S) of  $\sigma_1$  obtained from the focal mechanism solution diagrams of recent seismic events sourced from the major active faults in the eastern central Anatolia (Figure 1b). The minor difference between these two operation directions (N-S and NNE) can be attributed to a clockwise rotation, which is coeval with the development of the fissure-ridge travertines (Gürsoy et al., 1998; Tatar et al., 2000).

**4. Basin structures**

The most diagnostic structure in the study area is the Salanda depression. It is an approximately 1–9 km wide, 66 km long, and WNW (N65°W) trending, very young strike-slip basin developed on the erosional surface of the Ürgüp group during Quaternary time (Figures 4 and 9). The Salanda basin is drained by both the Kızılırmak River and its numerous subbranches flowing towards the depocenter of the basin. It is bounded by the Salanda master fault in the north and various discontinuous segments of the Tuzköy fault set in the south (Figures 4 and 9). Based on their ages and origins, the geological structures exposed in and adjacent to the Salanda basin are classified into two categories, namely the paleotectonic structures and the neotectonic structures. Paleotectonic structures are represented by reverse faults (Figure 10), closed to open folds that developed in both the Tuzköy Formation and the Ürgüp group (Figures 4 and 9). These are the real shortening structures that resulted from different compressive phases that operated at different times in the Eocene and Pliocene periods (Figure 2). These compressive phases were interrupted by several intervening short- to long-term tensional phases (Figure 2). The last phase of the tensional tectonic regime prevailed during late Middle Miocene-Pliocene time. It was accompanied by both the Central Anatolian volcanism and the contemporaneous fluviolacustrine sedimentation, which resulted in the CAVP and its major unit (the Ürgüp group). Starting from

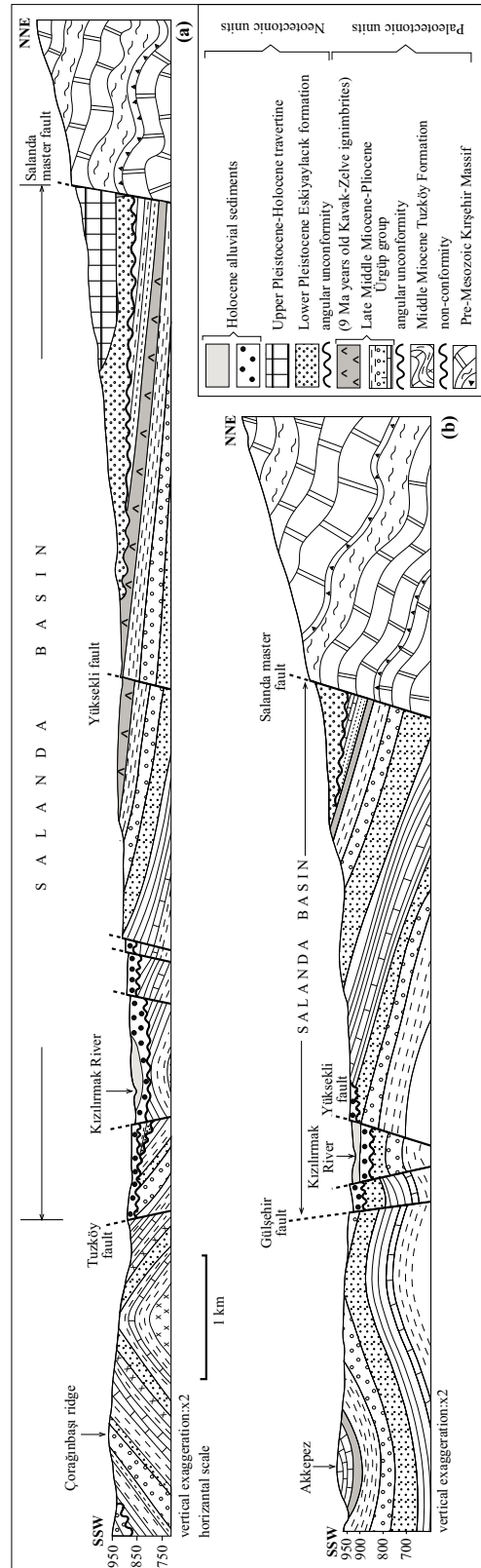


**Figure 9.** Geological cross-sections illustrating the outline of the Salanda strike-slip basin and the deformed pattern (folded pattern) of the paleotectonic units.

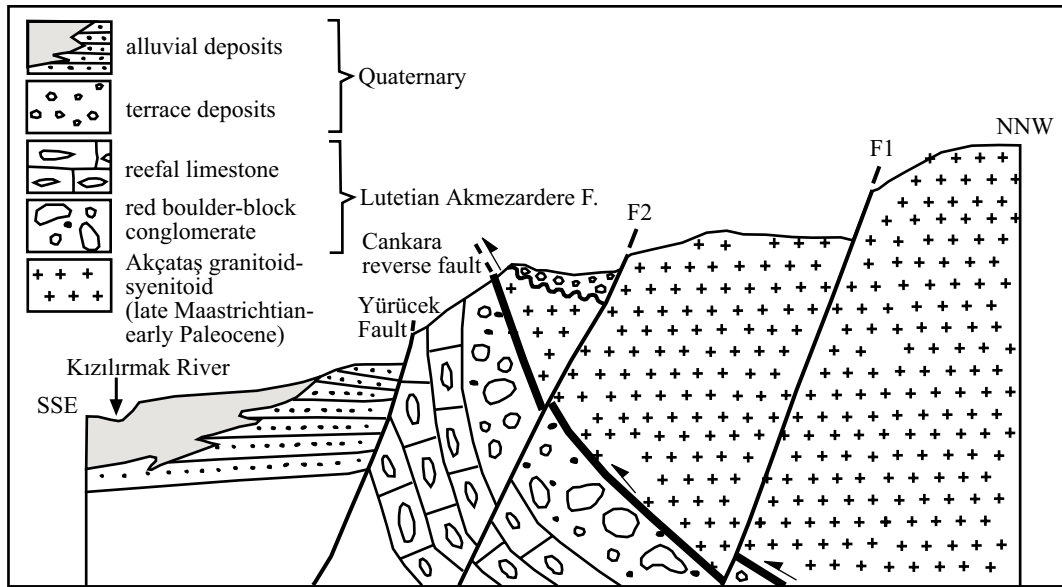


**Figure 10.** Sketched geological cross-section showing the reverse fault contact between the Akçataş granitoid-syenitoid and the Lutetian Akmezardere Formation (Ta), which is cut and displaced by the several fault segments that form the Salanda Fault Zone.

the early Quaternary onward, this last phase of tensional tectonic regime was interrupted again and then replaced by the strike-slip neotectonic regime. It resulted in the Salanda strike-slip basin and afterwards the settling of the Kızılırmak River into it. During this strike-slip neotectonic regime, on one side, some older structures inherited from the pre-Quaternary paleotectonic period (e.g., the Salanda master fault) have been reactivated, and on the other side, new faults constituting both the Salanda and Avanos Fault Zones were formed (Figures 4 and 9). The detailed description of the older paleotectonic structures is beyond the scope of the present paper. However, reactivated older faults and the neotectonic structures are explained below.

#### 4.1. Neotectonic structures

The existence of a very young basin and its northern margin-boundary fault (Salanda master fault) was first identified and reported by Koçyiğit (1984). Later on, a broader area, which also includes the Salanda basin, was interpreted and reported as a “graben” by Toprak (1994). He also interpreted its margin-boundary structures as normal faults. These studies were followed by several others (Atabey, 1998a, 1998b; Dhont et al., 1998; Froger et al., 1998). Atabey (1998a, 1998b) mapped a fault with a northward convex pattern in the area between Karadağ in the southeast and historical Kesikköprü in the west and then interpreted it as a normal fault. Later on, the same structure was renamed as the “Gümüşkent Fault” and then it was combined with the N-S trending Derinkuyu Fault by Dhont et al. (1998). Lastly, these authors interpreted

these two faults together with the NW trending “Salt Lake Fault” as the west-southwestward gently dipping and spoon-shaped tensional detachment faults. In contrast to the idea of these authors, our recent field data (the trace and dip amount of faults, ratio of the throw amount to the lateral offset, and the style of faulting) strongly imply strike-slip faulting and related pull-apart basin formation, not normal faulting and graben.

##### 4.1.1. Salanda Fault Zone

This is a zone of active deformation approximately 5–19 km wide, 180 km long, and WNW (N75°–80°W) trending located between Bala district in the northwest (outside the study area) and Avanos district in the southeast (Figures 1b and 4). Its 65-km-long southeastern section (the historical Kesikköprü Bridge-Avanos section) is included in the study area (Figure 4). The Salanda Fault Zone appears around the town of Afşar in the near south of Bala district in the northwest and then runs southeastward for 12 km in distance up to the near south of Kesikköprü town, where it intersects with the NNE trending Konya-Altınekin oblique-slip normal fault zone (Figure 1b). Starting from this area of intersection, it continues along the Kızılırmak River Valley in the same trend up to the historical Kesikköprü Bridge, where it enters the study area. Hereafter, the Salanda Fault Zone runs towards the ESE for about 65 km in distance, intersects with the ENE trending Avanos Fault Zone, and then terminates there (Figure 4). In general, the Salanda Fault Zone consists of numerous short to long (1.6–23 km) and closely-spaced

(0.2–3 km) structural fault segments and fault sets. Most of them trend in the WNW direction while a limited number of fault segments trend in N-NE and E-W directions, respectively. The most significant single faults and the fault sets forming the Salanda Fault Zone are the Salanda, Yürücek, and Hırkadağ single faults and the Tuzköy to Karadağ fault sets (Figure 4).

The Salanda single fault is the master structure of the Salanda Fault Zone. It is the most outstanding structure inherited from the paleotectonic period. It determines and controls the north-northeastern margin of the Salanda basin. The Salanda master fault appears approximately 1 km north of the Avanos district at the southeast tip of the Salanda basin and then runs in a NW trend for about 15 km in distance up to the Kızılöz Stream, where it is crosscut and offset sinistrally for about 4.2 km by the NE trending Yeşilöz fault (Figure 4). The Salanda master fault reappears in the west of Yeşilöz village and then continues in a WNW trend for about 10 km in distance up to Ağralının Hill, where it jumps towards the north by about 2 km. Hereafter, it follows the same trend in the west-northwest direction up to the near east-southeast of the Avcıköy settlement, where it bifurcates into four subbranches and then exits the study area at the northwest tip of the Salanda basin (Figure 4). Both the paleotectonic rock assemblages (metamorphic rocks of the Kırşehir Massif, Akçataş granitoid-syenitoid, Lutetian Akmezardere Formation) and the Quaternary neotectonic basin fill (Eskiyaylacık formation, Karaburna olivine basalt and travertine occurrences) are crosscut, displaced in both vertical to right lateral directions, and then tectonically juxtaposed to each other by the Salanda

master fault (Figure 4). For example, the contact between the Lutetian Akmezardere Formation and the Karaburna basalt flow of 1.228 Ma old is cut and displaced up to 5 km in the right lateral direction by the Salanda master fault (X-X in Figure 4). In the same way, the Karaburna basalt flow is also cut and displaced up to 43 m in the vertical direction by the Salanda master fault (Z in Figure 4). Thus, the ratio of the throw amount (43 m) to the lateral offset (5 km) accumulated on the master fault during the last 1228 ka strongly reveals that the Salanda master fault is of a strike-slip character rather than of a normal fault nature. A sudden break in slope, triangular facets deflected to offset streams, intensely crushed brecciated and sheared fault rocks, secondary calcite mineral growth, and the well-developed to preserved slickenside with superimposed sets of slickenlines (Figure 11a) are the most diagnostic morphotectonic and fault plane-related criteria that indicate the existence and the strike-slip nature of the Salanda master fault. The Salanda master fault was originally a normal fault. It controlled the sedimentation and accumulation of the Ürgüp group during the late Middle Miocene-Pliocene. This is proven by the kinematic analysis of the slip-plane data (Figure 11b) measured on slickenside at station S-1 (S-1 in Figure 4). However, it was reactivated as a dextral strike-slip fault during the Quaternary neotectonic period. This is indicated by both the slickensides with the overprinted sets of nearly horizontal slickenlines and the actively growing fissure-ridge travertine occurrences (Kızıltepe, Salanda, and Balkaya-Boztepe fissure-ridge travertines) aligned parallel to the trace of the Salanda master fault (Figures 8a–8c).

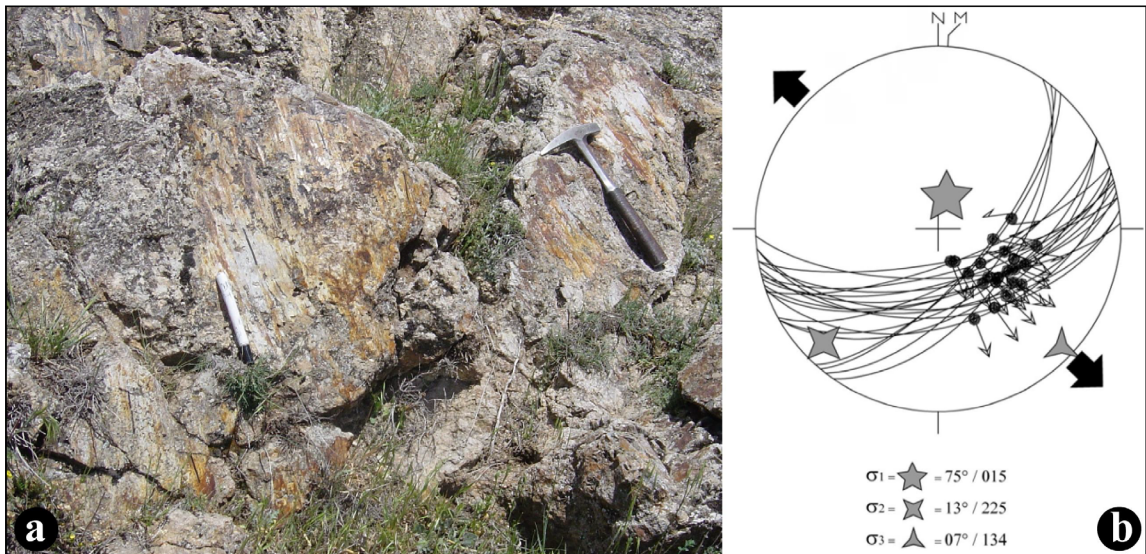


**Figure 11.** a) Close-up view of the Salanda master fault slickenside at station 1 (S-1 in Figure 1). b) Stereographic plot of slip-plane data on the Schmidt lower hemisphere net (large diverging black arrows show local extension direction during the extensional paleotectonic period).



Their long central fissures trend between N10°E and N30°E and run parallel to the local operation direction of the major principal compressive stress ( $\sigma_1$ ). This result also fits well with the regional operation direction of  $\sigma_1$  obtained from the focal mechanism solution diagrams of destructive earthquakes that occurred in East Central Anatolia (Figure 1b). As a matter of fact, both the Afşar and Bala fault segments, which form the northwest tip of the Salanda Fault Zone in the further northwest, were activated and caused the 31 July 2005 and 23 December 2007 earthquakes of  $M_l = 5.2$  and  $5.6$ , respectively (Koçyiğit, 2009; Tan et al., 2010). Their focal mechanism solution diagrams show that the operation direction of the major compressive stress ( $\sigma_1$ ) is approximately N-S (Figure 1b). However, the rest of the longer eastern part of the Salanda Fault Zone is still of the nature of a seismic gap.

Another significant structure forming the Salanda Fault Zone is the Yürücek fault. It is a NW trending strike-slip fault of 20 km long located at the northwestern tip of the Salanda basin. The Akçataş granitoids of late Maastrichtian-early Paleocene age and the Lutetian Akmezardere Formation are crosscut, displaced in vertical and lateral directions, and then tectonically juxtaposed with the Holocene alluvial sediments by the Yürücek fault (Figure 12a). The intensely crushed to brecciated fault rocks and tectonic juxtaposition of older and younger units along the linear fault trace are common morphotectonic criteria for recognition of this fault. The Yürücek fault also displays a well-preserved slickenside (Figure 12b) with a set of nearly horizontal slip-lines on the granitoid in places (S-2 in Figure 4). They indicate a dextral strike-slip faulting with a considerable amount of dip-slip component.

The Hırkadağ fault is a dextral strike-slip fault that is approximately 25 km long, WNW trending, and northerly steeply dipping. It is located in the area between the Çoğlu settlement in the northwest and the NE trending Yeşilöz fault in the southeast (Figure 4). It determines the north-northeastern foot of the Hırkadağ structural high or pressure ridge. Both the older basement rocks (metamorphic rocks of the Kırşehir Massif and the Upper Maastrichtian-Lower Paleocene Akçataş granitoid-syenitoid) and their Lutetian to Middle Miocene cover sequences (the Akmezardere and the Tuzköy formations) are crosscut and displaced up to 3.4 km in right lateral directions by the Hırkadağ fault (Y-Y in Figure 4).

Apart from these three northern margin-boundary single faults, there are also some other single faults, such as the Yüksekli and Avanos faults, developed inside the basin (Figure 4). These are the closely spaced, diversely sized (ranges from outcrop scale to several kilometers in length), and WNW trending strike-slip fault segments. A sudden break in slope and uplifted and fault-suspended

Quaternary terraces are diagnostic morphotectonic evidence of these fault segments. In the area between the Yeşilli and Hacılar settlements, one of the terrace deposits of late Pleistocene age (T8 in Figure 6) is sheared by these two fault segments. Their compressive effect on the terrace deposits was recorded as three outcrop-scale reverse faults (Figure 13a). The 22-km-long Yüksekli and the 16-km-long Avanos faults are the longest segments formed inside the basin. Both older rocks (the Tuzköy Formation and the Ürgüp group) and the Quaternary neotectonic basin fill are crosscut and tectonically juxtaposed to each other by the Yüksekli and Avanos faults (Figures 4 and 9).

#### 4.1.2. Tuzköy fault set

A series of closely spaced, diversely sized (1.6–19 km long), WNW to E-W trending and northerly steeply dipping to subvertical fault segments occur in a zone of deformation along the south-southeast margin of the Salanda basin (Figures 4 and 9). This fault zone segment is here termed the Tuzköy fault set. It determines and controls the southern margin of the Salanda basin in the area between near to the south of the Avanos district in the east and Karaboğaz village in the northwest (Figure 4). The Tuzköy Formation, the Ürgüp group, and various lithofacies of the Quaternary basin fill are crosscut, displaced in both vertical and lateral directions, and tectonically juxtaposed to each other by fault segments of the Tuzköy fault set (Figure 4). A series of fan-delta deposits occur at the foot of the Tuzköy fault set. Their original triangular shapes have been degraded, flattened, and aligned parallel to the general trend of the fault segments due to the motion along the active fault segments. In addition, a series of outcrop-scale reverse faults have developed owing to the compressive effect of the strike-slip faulting that occurred inside the Tuzköy fault set in the near northwest of the Gülşehir district located at the southeastern margin of the Salanda strike-slip basin (S-3 in Figure 4). One of these outcrop-scale reverse faults cuts across the underlying folded Ürgüp group and the unconformably overlying Quaternary basin fill (both the T15 terrace deposits and the overlying 96,000-year-old Karnıyarıktepe basalt) and then displaces them up to 20 m in a vertical direction (Figure 13b). Consequently, the flattened fan-deltas, uplifted and fault-suspended terraces, tectonic juxtaposition of Holocene alluvial sediments with older lithofacies, the fault deflected to a controlled drainage system such as the Kızılırmak River, and the very young (late Pleistocene) outcrop-scale reverse faults are diagnostic morphotectonic to fault plane-related criteria that indicate both the existence and activeness of some fault segments constituting the Tuzköy fault set.

#### 4.1.3. Karadağ fault set

Seven closely spaced and diversely sized (2–11 km) fault segments are exposed around Karadağ Hill at the southeastern margin of the Salanda basin (Figure 4). These

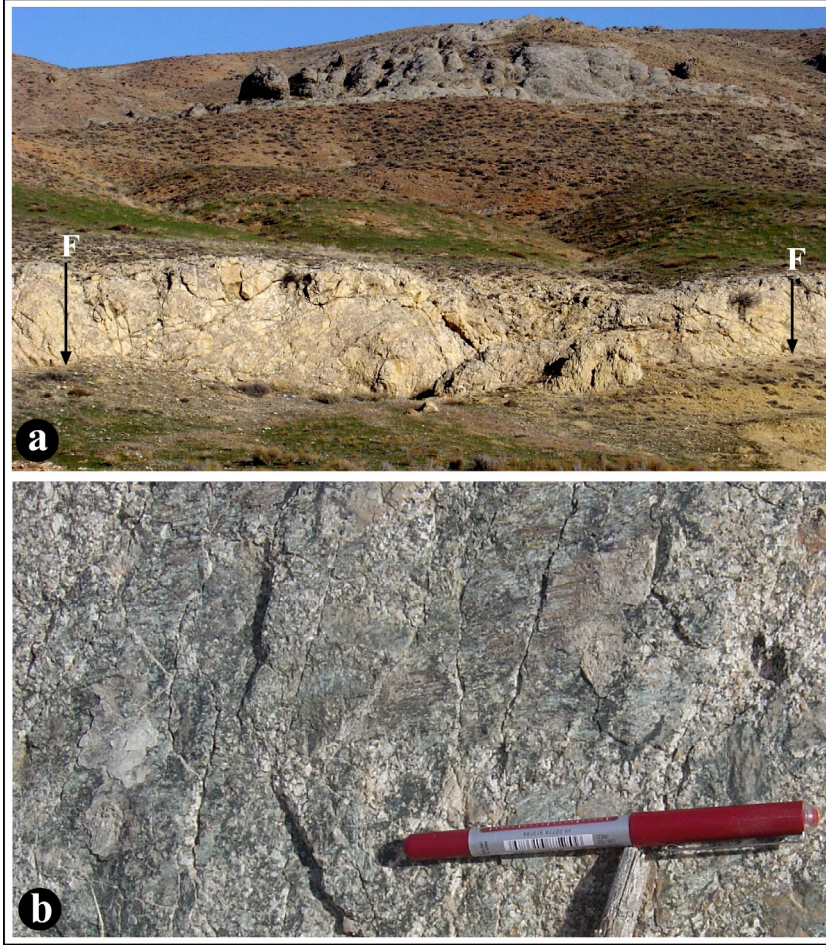


**Figure 12.** a) General view of the Yürücek fault (F-F) (near east of the historical Kesikköprü bridge, view to N). b) Close-up view of the Yürücek fault slickenside on the granitoid at station 2 (S-2 in Figure 4).

fault segments were previously mapped and named as the Karadağ Fault Set and then interpreted to be a normal fault by Toprak (1994). The same name is preserved in the present paper. Three of these fault segments, located on the northern side of the hill, trend WNW and dip steeply towards the north-northeast while the other four segments located at the southern side of the hill trend ENE and dip towards the south. These seven fault segments intersect with each other at the eastern foot of the Karadağ Hill and display a horse tail-like structural pattern. Indeed the northern three segments are parallel to the general trend of the Salanda Fault Zone to which they belong, whereas the southern fault segments are included in the Avanos Fault Zone (Figure 4). All these fault segments are crossed and displaced up to 4 km in the right lateral direction by the WNW trending fault included in the Salanda Fault Zone (Figure 4). One of the southerly dipping four fault segments (Sulusaray Fault) is exposed near the peak of the hill. It displays a well-developed and preserved slickenside

(S-4 in Figure 4 and Figure 14a). Their kinematic analysis reveals that this fault segment was originally a normal fault (Figure 14b). However, all of the fault segments forming the Karadağ fault set were originally the same in age, and then they were reactivated all together as strike-slip faults during the Quaternary neotectonic period. This is evidenced by the actively growing Karadağ fissure-ridge travertine occurrence offset in both the dextral and sinistral directions by the conjugate fracture system filled by volcanic clast-rich travertine.

#### 4.1.4. Avanos Fault Zone

This is the second major structure exposing in and near the northeast and also outside the study area. Indeed, it is one of the active sinistral strike-slip fault zones forming the Central Anatolian Fault System (Koçyiğit and Beyhan, 1998). The Avanos Fault Zone is a approximately 6–9 km wide, 98 km long, and ENE to NE trending, a zone of deformation located between Avanos in the southwest and Lake Tuzla (outside the study area) in the northeast

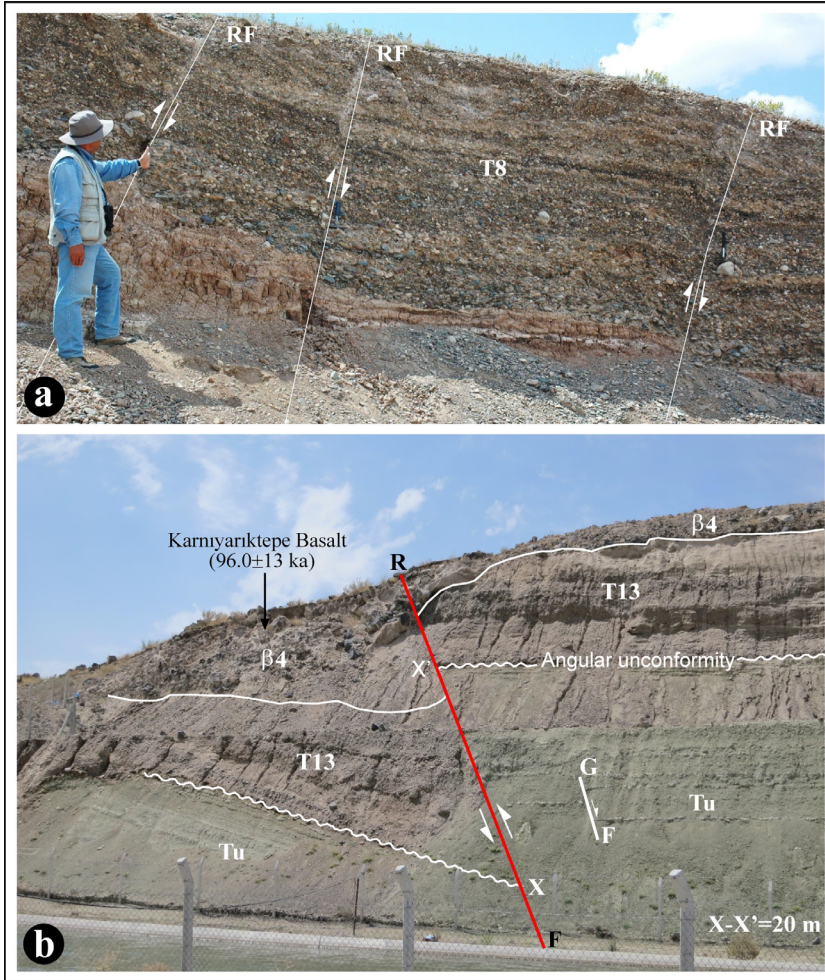


**Figure 13.** a) Close-up view of the outcrop-scaled reverse faults (RF) cutting across the terrace deposits (T8) in Yeşilli village. b) General view of the mapable reverse fault (RF) at station 3 (S-3 in Figure 4), which cuts both the Upper Middle Miocene-Pliocene Ürgüp group (Tu), the unconformably overlying modern basin fill (T13), and Karnıyarıktepe fissure basalt flow ( $\beta$ -4) and displaces them up to 20 m in a dip-slip direction (X-X'). GF: Normal type of growth fault developed in the older Ürgüp group.

(Figure 1b). Both the Salanda and Avanos Fault Zones intersect each other at the southeastern tip of the Salanda basin and control it (Figure 4). The Avanos Fault Zone begins to appear as several fault segments exposed at the southern side of the Karadağ Hill in the southwest and then continues in the ENE direction along the Kızılırmak River Valley up to the near north of Lake Tuzla, where it joins with the master fault of the Central Anatolian fault system and then terminates (Figures 1b, 4, and 15). As a natural response to the weakness and motion of the Avanos Fault Zone, the Kızılırmak River has incised deeply into its bed, resulting in a narrow gorge at the elevation of 975 m below the peak elevation of 1500 m of the surrounding mountains such as Kocadağ and Allıdağ (Figure 15). Only the 35-km-long southwestern section (Kocadağ-Karadağ

section) of the Avanos Fault Zone is included in the study area (Figures 4 and 15). It consists of numerous short to long (2–30 km), closely to medium-spaced (0.5–4 km) and predominantly ENE trending but also NW to N-S trending fault segments. The common criteria used to recognize the fault segments forming the Avanos Fault Zone are a sudden break in slope; triangular facets; intensely crushed to brecciated fault rocks; tectonic juxtaposition of older rocks with the Quaternary neotectonic basin fill; offset formation boundaries; uplifted, dissected, and fault-suspended terrace deposits; fault-parallel aligned hot water springs; fissure-ridge travertine occurrences (Sarıhıdır, Bayramhacılı, and Tekgöz thermals and travertines); the deflected to offset drainage system; and the eruption center of the Quaternary olivine basalt. The

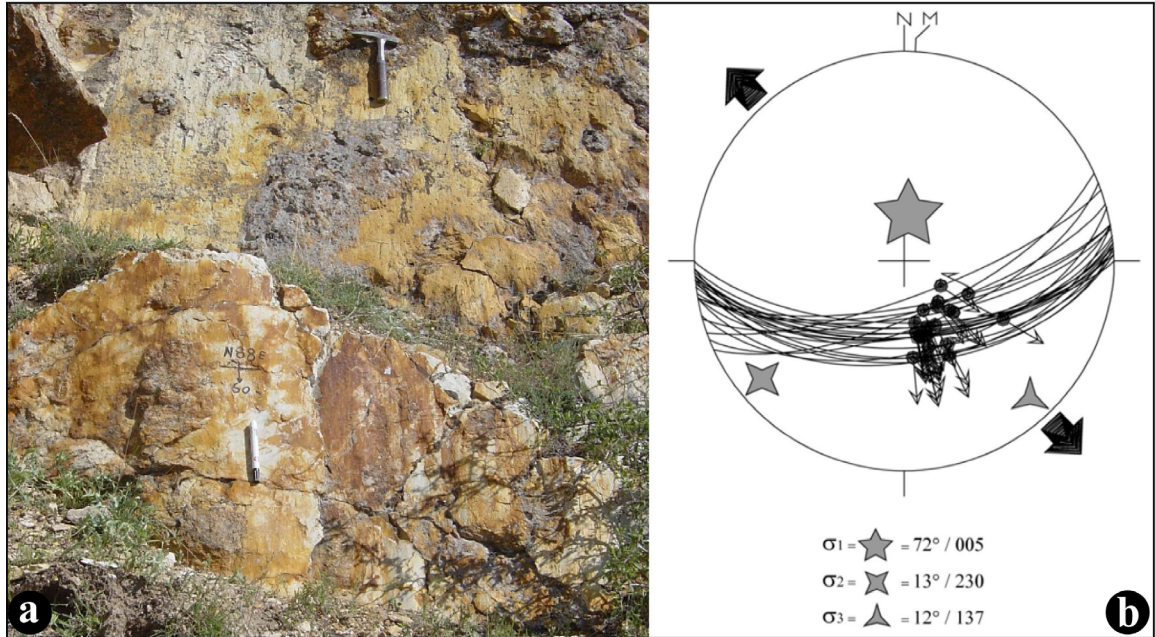


**Figure 14.** a) Close-up view of the Karadağ fault slickenside at station 1 (S-4 in Figure 4). b) Stereographic plot of slip-plane data on the Schmidt lower hemisphere net (large diverging black arrows indicate local extension direction in the extensional paleotectonic period).

major segments forming the Kocadağ-Karadağ section of the Avanos Fault Zone are, from north to south, the Bozca, Sarıhıdır, Esebağı, Küllü, Çavuşin. and Karahüyük faults (Figures 4 and 15).

The Bozca and Karahıdır faults are the northern margin-boundary faults of the Salanda basin. They are more or less similar in length (30 km) and trend in the NE direction. In the area between the Tekgöz thermals in the northeast and the Avanos district in the southwest, various older rocks and neotectonic basin fill are crosscut and displaced in both vertical and lateral directions and tectonically juxtaposed to each other by these two faults (Figures 4 and 15). Particularly, in the south of Yuvalı village, the boundary between the Middle Miocene basaltic volcanics and younger Ürgüp group is cut and displaced (up to 9 km) in the left lateral direction by the Sarıhıdır fault (Figure 15). In addition, the Sarıhıdır fault also determines and controls the northern outline of the Kızılırmak River flood plain.

The Küllü and Esebağı faults occur as two separate segments of 15 km and 11 km in length, respectively, inside the basin. They are northerly steeply dipping sinistral strike slip faults located between the Tekgöz thermal area in the northeast and Avanos in the southwest (Figures 4 and 15). They determine and control the southern outline of the Kızılırmak River floodplain. The older Ürgüp group, the Quaternary terraces, fan-delta deposits, and recent alluvial sediments are crosscut, displaced in both vertical

to lateral directions, and tectonically juxtaposed to each other by these two faults.

In the near south-southeast of Bozdağ, the Kocadağ fault, which is the master fault of the Avanos Fault Zone, bifurcates into two subbranches and results in a highland (Sofular pressure ridge) bounded by them. They are here termed as the Çavuşin and Karahüyük faults (Figure 15). They determine and control the southern margin of the Salanda basin. Both the Çavuşin and the Karahüyük faults run in a WSW direction for about 26 and 24 km in distance, respectively, up to the Çavuşin settlement, where they are cut and displaced for about 4 km in the right lateral direction by a WNW trending fault segment included in the Salanda Fault Zone. Lastly, they rebifurcate into four fault segments and then form the Karadağ fault set located further southwest (Figure 4). Various lithofacies of the Ürgüp group of late Middle Miocene-Pliocene age and the Quaternary terrace deposits exposed at the southern side of the Kızılırmak River gorge are crosscut, displaced in vertical and lateral directions, and tectonically juxtaposed to each other by both the Çavuşin and Karahüyük faults. A sudden break in slope amount, triangular facets, deflected to offset drainage system, crushed to sheared strips of rocks, fault-parallel pressure ridges (e.g., the Sofular and Karakaya pressure ridges), and the slickenside with the overprinted sets of slip-lines are the most common morphotectonic and fault plane-related criteria observed and used to recognize these two faults.

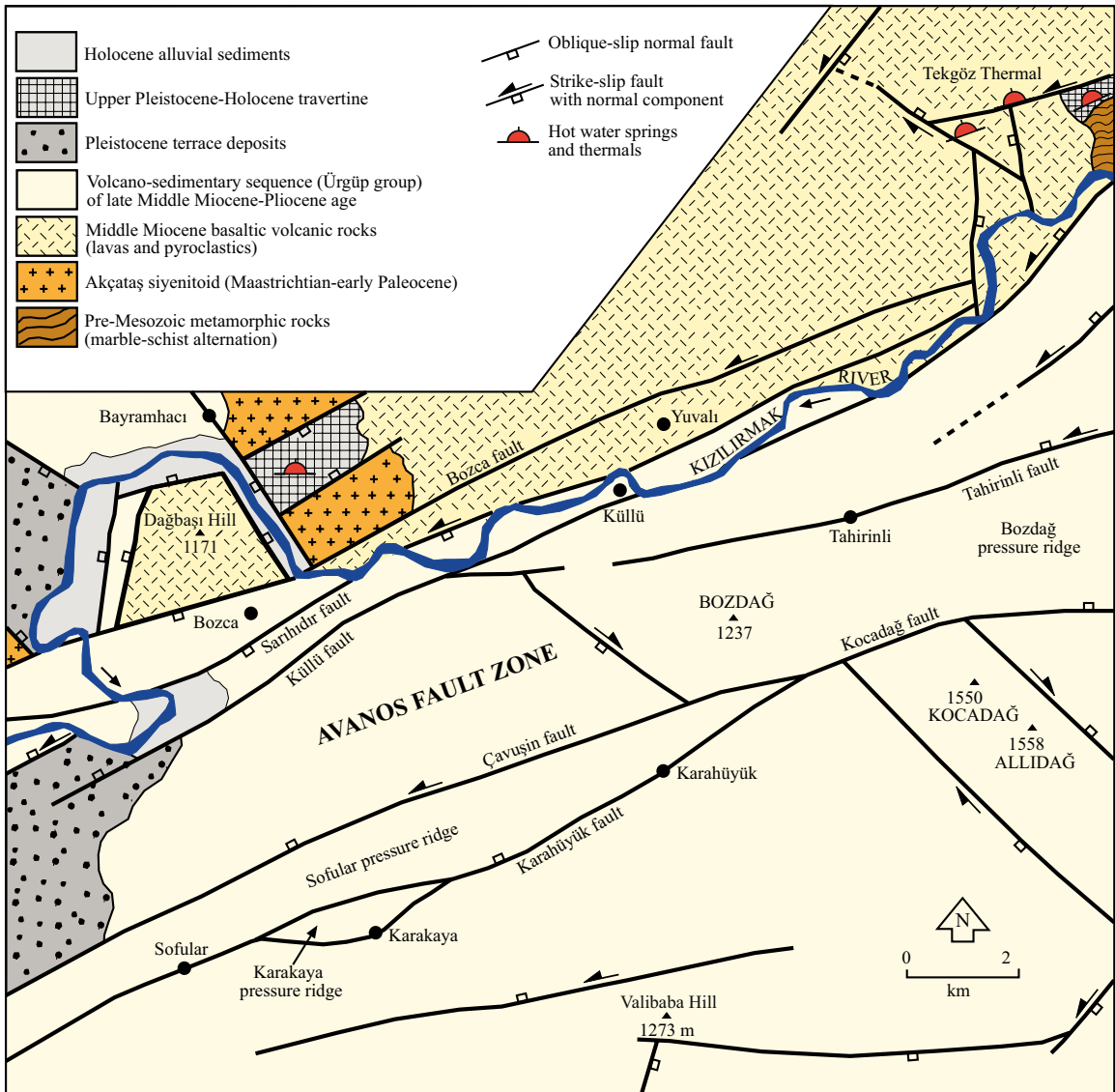


Figure 15. Geological map of the Kocadağ-Sofular section of the Avanos Fault Zone.

### 5. Discussion and evolutionary history of Salanda basin

In the west of Cyprus, a NNE-directed slow subduction between the Anatolian platelet and the African plate is still active (Robertson and Grasso, 1995). In contrast to this, in the east of Cyprus, the northward motion of the Arabian Plate with respect to the African Plate was restricted by the late Middle Miocene terminal suturing of the Arabian Plate with the Eurasian Plate until the late early Pliocene (Hempton, 1987; Koçyiğit and Beyhan, 1998; Koçyiğit et al., 2001). During this time interval, this region experienced a long-term postcollisional continental convergence and related strain (McKenzie, 1969). Accordingly, in the same time slice, a widespread calc-alkaline volcanic activity and fluvio-lacustrine sedimentation occurred in the Central Anatolia (Ercan, 1986; Notsu et al., 1995). They resulted

in a thick pile of volcanosedimentary sequence termed as the Ürgüp group in the present paper. The Ürgüp group is the main and widespread paleotectonic rock unit of the CAVP. It is penetrated by several stratovolcanoes and numerous monogenetic centers (basaltic to felsic maars, cinder cones, and silicic domes) that originated from the Central Anatolian Volcanic Arc (Pasquare et al., 1988; Toprak, 1998, Koçyiğit and Erol, 2001). However, during the Quaternary, several large andesitic-basaltic stratovolcanoes including a number of monogenetic igneous centers in the nature of fissure eruptions developed. They strongly reveal both an inversion in the nature of magmatic activity and the onset of a new tectonic regime in the Cappadocia region (Keller, 1974; Pasquare et al., 1988). The CAVP was originally a NE-SW trending

continuous depression bounded and controlled by a series of ENE trending normal faults during the late Middle Miocene-Pliocene paleotectonic period (Pasquare et al., 1988). One of the major extensional structures that took part in the development of the CAVP is the Salanda master fault. Indeed, it was an originally oblique-slip normal fault during the paleotectonic period. This is evidenced by the fault slickensides and the kinematic analysis of slip-plane data measured on them (Figures 11 and 14). This kinematic analysis also reveals that the extension was operating in the NW-SE direction during the late Middle Miocene-Pliocene paleotectonic period. However, the Salanda master fault was rotated into its present-day position and then reactivated as the strike-slip fault during the Quaternary neotectonic period (Figure 16) (Gürsoy et al., 1998; Platzman et al., 1998; Tatar et al., 2000). Even if some previous studies (Toprak and Göncüoğlu, 1993; Toprak, 1994, 1996; Köksal and Göncüoğlu, 1997; Dhont et al., 1998; Dirik et al., 1999; Dirik, 2001; Özsayın et al., 2013) reported that this tensional tectonic regime is continuous from the late Middle Miocene to recent time, this is not true because it was interrupted and replaced by a strike-slip neotectonic regime at the end of the latest Pliocene or more probably the early Quaternary (Figure 16). This is evidenced by a series of field data: 1) the regional angular unconformity between the underlying deformed paleotectonic fill of late Middle Miocene-Pliocene age and the overlying nondeformed neotectonic fill of Quaternary age; 2) some fault segments forming the Salanda Fault Zone display fault slickensides with two sets of overprinted slip-lines where the younger set is a strike-slip in origin (Figure 12b); 3) a series of well-developed fissure-ridge type of travertines with the long central axes trending in the NNE and running parallel to the operation direction of the major principal compressive stress ( $\sigma_1$ ) in the CAVP; 4) the northwestern section (the Bala section) of the Salanda Fault Zone was reactivated and resulted in two recent earthquakes (the 31 June 2005 and 20 December 2007 Bala earthquakes), whose focal mechanism solution diagrams (Koçyiğit, 2009; Tan et al., 2010) reveal a strike-slip tectonic regime, in which the  $\sigma_1$  is also operating in an approximately N-S direction (Figure 1b); 5) the occurrence of three sets of intersecting systematic fractures, which cut across the actively growing Karadağ travertine and offset each other in both dextral and sinistral directions, revealing the existence of a strike-slip tectonic regime in the region; 6) a widespread occurrence of the outcrop-scaled and mappable reverse faults that cut and displaced both the older Ürgüp group rocks and the overlying Quaternary basin fill (terrace deposits and basalt flows) up to 20 m; 7) both the stratigraphical and geographical markers, such as the formation boundaries and drainage system, are offset up to 5 and 9 km in dextral and sinistral

directions, respectively; and 8) the total throw amount accumulated on the southern margin-boundary faults of the Salanda basin is approximately 178 m, which is small compared with the total amount of dextral strike-slip displacement (5 km) accumulated on the Salanda Fault Zone. Consequently, on one hand, early-formed tensional structures have been reactivated as strike-slip faults, and on the other hand, some new faults, such as the Avanos Fault Zone and the Tuzköy fault set (Figures 15 and 16) have formed. Thus, starting from the early Quaternary onwards, the CAVP began to experience a strike-slip tectonic regime, and then it was divided into several strike-slip basins of dissimilar size and origin (Figure 16). One of the well-developed examples of these depressions is the Salanda strike-slip basin. It was previously reported as a graben bounded by normal faults (Toprak, 1994). In contrast, it is approximately 1–9 km wide, 66 km long, and WNW (N65°W) trending, a lenticular strike-slip basin located between the historical Kesikköprü in the west and the Sarıhıdır settlement in the east. It is drained by the longest (1355 km) antecedent drainage system, the Kızılırmak River, in Turkey (Figure 4).

The Salanda basin began to develop on a regional late Pliocene erosional surface underlain by the deformed (folded) Ürgüp group in the northern section of the CAVP under the control of a strike-slip neotectonic regime dominated by both the Salanda and Avanos Fault Zones (Figure 16). The oldest sedimentary pile accumulated in the Salanda strike-slip basin is the Eskiyaylacık formation. It is a fluvial sedimentary sequence deposited in a setting of alluvial fan by a drainage system with both southerly and northerly located transverse tributaries. The Eskiyaylacık formation is nearly flat-lying (nondeformed) and overlies with an angular unconformity the whole of the deformed (folded to faulted) rocks of pre-Quaternary age at the bottom, and then it is succeeded conformably by the alternation of terrace deposits and basalt flows (Figures 3 and 5b). The oldest terrace deposit (T1 in Figure 6) occurs at an elevation of 160 m above the current bed of the Kızılırmak River along the southern margin of the Salanda basin and is capped and fossilized by the Evren Ridge basalt flow, 1.989 Ma old, while the other terraces (T2 and T4 in Figure 8a) are exposed at elevations of 138 m, 130 m, and 120 m, respectively, along the northern margin and capped by the Karaburna basalt flows of 1.228 Ma old. Thus, both the Eskiyaylacık formation and the overlying oldest terrace (T1) must be at least an approximately 2 Ma in age or a little older. The basalt flows were poured out of the earth's surface as fissure-ridge eruptions from centers located on both the southern and northern margins of the Salanda basin (Figure 4). These data strongly reveal that the Kızılırmak River had just settled into the Salanda basin during the Early Quaternary (~2.6 Ma BP) and then

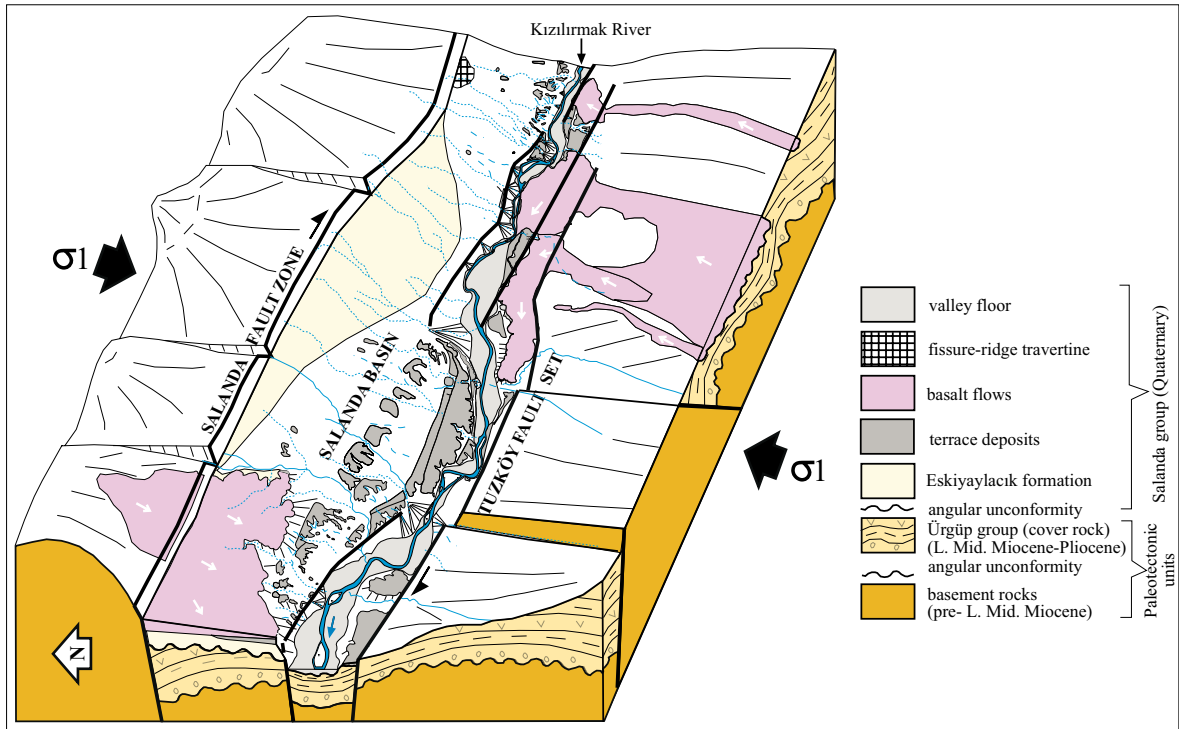


**Figure 16.** A summary sketched block diagram depicting the evolutionary history of the Salanda pull-apart basin (large converging bold arrows indicate operation direction of principal compressive stress in the study area).

it was followed by basaltic fissure eruptions related to the margin-boundary faults (Doğan, 2011). The modern basin fill continues upward with a series of terraces (T5 through T15) and intervening several basaltic flows (the Tuzköy basalt flow, 404 ka years old, and the Karnıyarıktepe basalt flow, 96 ka years old) capped by fissure-ridge travertine occurrences at the topmost (Figure 3). The T15 and the Karnıyarıktepe basaltic flow are the youngest terrace deposit and lava flow respectively observed at the southern margin of the Salanda strike-slip basin (Figures 4 and 6). Their contact is exposed at an elevation of 4.5 m above the current bed of the Kızılırmak River. The maximum relief between the oldest (T1) and the present valley floor is about 160 m and this value corresponds to the total vertical incision of the Kızılırmak drainage system as a natural response to the tectonic uplift until the present time. In addition, both the underlying older Ürgüp group and the overlying modern basin fill (the T13 and the Karnıyarıktepe basalt flow) are cut and displaced (up to 20 m) by a mappable reverse fault that resulted from the strike-slip complexity along the southern margin (S-3 in Figure 4). This observation indicates that the strike-slip faulting was also operating during the late Pleistocene. The topmost part of the modern basin fill consists mostly of fissure-ridge travertines of late Pleistocene-Holocene age (Temiz et al., 2009). They grade into coarser-grained alluvial fans and fan-apron deposits in both lateral and

vertical directions and have a mean central axis trending in the NNE direction. Fissure-ridge travertines are also strike-slip faulting-induced extensional structures and their long central axes run more or less parallel to the operation direction of the major principal compressive stress ( $\sigma_1$ ), which controlled their development. This is also proven by the focal mechanism solution diagrams of the 18 April 1938 Akpınar (Kırşehir), the 31 June 2005 and 20 December 2007 Bala, and the 1 January 2016 Hacıduraklı (Çiçekdağı-Kırşehir) earthquakes (Tan et al., 2010; USGS, 2016) (Figure 1b), i.e. the Salanda basin is actively growing under the control of a strike-slip neotectonic regime, not a tensional tectonic regime as reported in some previous works (Toprak and Göncüoğlu, 1993; Toprak, 1994, 1996; Köksal and Göncüoğlu, 1997; Dhont et al., 1998; Dirik et al., 1999; Dirik, 2001; Özsayın et al., 2013)

## 6. Conclusions

Based on both data presented in the previous sections and the discussions carried out just above, we draw the following conclusions: 1) triangular-shaped Central Anatolia, which includes both the CAVP and the study area (the Salanda strike-slip basin), was under the control of a tensional tectonic regime (last paleotectonic regime) until the end of late Pliocene; (2) starting from the early Quaternary (~2.6 Ma BP) onwards, the last tensional tectonic regime and related faults were replaced by a

strike-slip neotectonic regime and related structures; 3) the major principal compressive stress ( $\sigma_1$ ) is operating in an approximately NNE direction as indicated by both the fissure-ridge travertines and focal mechanism solutions of earthquakes that occurred in Central Anatolia; 4) the CAVP was crosscut and dissected into several depressions as a natural response to the strike-slip neotectonic regime; 5) one of these depressions is the Salanda strike-slip basin, 6) which is not a graben but in fact is a lenticular strike-slip basin located in the northern section of the CAVP; 7) in the present this basin continues to develop under the control of a strike-slip neotectonic regime based on both the stratigraphical data (the regional angular unconformity between older and modern basin fill) and the structural data such as the fissure-ridge travertines, basaltic flows of fissure eruption's origin, outcrop-scaled to mappable reverse faults cutting across the older to modern basin fills, the earthquakes of strike-slip faulting origin, and the very small ( $\sim 0.03$ ) ratio of throw amount (178 m) to the dextral strike-slip offset (5 km) accumulated on the master faults; 8) the oldest rock unit of the modern basin fill accumulated in the Salanda basin represents a fluvial sequence (Eskiyaylacık

formation) succeeded by the alternation of 15 terraces and the intervening fissure-ridge basalt flows of early-late Quaternary age; 9) the fluvial Eskiyaylacık formation and overlying oldest terrace deposits (T1) are conformably overlain by the 1.989-Ma-old Evren Ridge basalt flow, i.e. these fluvial sedimentary piles deposited by the Kızılırmak drainage system and the eruption of basalts are more or less the same in age; 10) this short time slice can be bracketed between the Valibabatepe Ignimbrite of 2.52–3.0 Ma old from the bottom and the Evren Ridge basalt flow of 1.989 Ma old from the top. Thus, the first settling of the Kızılırmak River into the Salanda modern basin occurred in a time slice after the accumulation of the Valibabatepe Ignimbrite but before the eruption of the Evren Ridge basalt. This is one of the key events implying the onset of the strike-slip neotectonic regime in CAVP.

### Acknowledgments

This study was partly supported by the Scientific and Technological Research Council of Turkey (TÜBİTAK), Project Number 112Y153, and Informatic Engineering (BM), Project Number 07-03-09-1-00-23.

### References

- Akgün F, Olgun E, Kuşçu I, Toprak V, Göncüoğlu MC (1995). New findings on the stratigraphy, sedimentology and true age of the "Oligo-Miocene" cover of the central Anatolian Complex. *TAPG Bull* 6: 51-68.
- Altunel E (1996). Pamukkale travertenlerinin morfolojik özellikleri, yaşları ve neotektonik önemleri. *MTA Dergisi* 118: 47-64 (in Turkish).
- Altunel E, Hancock PL (1993). Active fissuring and faulting in Quaternary travertines at Pamukkale, western Turkey. *Z Geomorphol* 94: 285-302.
- Altunel E, Karabacak V (2005). Determination of horizontal extension from fissure-ridge travertines: a case study from the Denizli Basin, southwestern Turkey. *Geodin Acta* 18: 333-342.
- Atabey E (1989a). Aksaray-H18 Quadrangle, 1:100,000 Scale Geological Map and Explanatory Text. Ankara, Turkey: MTA Publications (in Turkish with an abstract in English).
- Atabey E (1989b). Aksaray-H19 Quadrangle, 1:100,000 Scale Geological Map and Explanatory Text. Ankara, Turkey: MTA Publications (in Turkish with an abstract in English).
- Aydar E, Schmitt AK, Çubukçu HE, Akın L, Ersoy O, Şen E, Duncan RA, Atıcı G (2012). Correlation of ignimbrites in the central Anatolian volcanic province using zircon and plagioclase ages and zircon compositions. *J Volcanol Geoth Res* 213-214: 83-97.
- Aydın SN (1991). Petrographic characteristics of the central Anatolian Massif Akçataş granite (Nevşehir). *Bull Min Res Exp* 112: 117-133.
- Batum İ (1978). Geology and Petrology of Acıgöl and Göllüdağ Volcanics at Southwest of Nevşehir (Central Anatolia/Turkey). *Yerbilimleri Dergisi* 4: 70-88.
- Beekman PH (1966). The Pliocene and Quaternary volcanism in the Hasan Dag-Melendiz Dag region. *Bull Min Res Exp* 66: 90-105.
- Besang C, Eckhardt FJ, Harre W, Kreuzer H, Müller P (1977). Radiometrische Altersbestimmungen an Neogenen Eruptivgesteinen der Türkei. *Geologisches Jahrbuch* 25: 3-36 (in German).
- Blumenthal M (1941). Niğde ve Adana vilayetleri dolayındaki Torosların jeolojisine umumi bir bakış. MTA Yayınları Seri B6. Ankara, Turkey: MTA (in Turkish).
- Boztuğ D, Güney O, Heizler M, Jonckheere RC, Tichornirowa M, Otlu N (2009). 207 Pb-206 Pb, 40 Ar-39 Ar and fission-track geothermochronology quantifying cooling and exhumation history of the Kaman-Kırşehir region intrusions, Central Anatolia, Turkey. *Turkish J Earth Sci* 18: 85-108.
- Broggi A, Capezzuoli A, Costantini A, Gandin A, Lazzarotto A (2005). Tectonics and travertines relationship in the Rapolano Terme area (Northern Apennines, Italy). In: *Proceedings of the First International Symposium on Travertine*, pp. 142-148.
- Dhont D, Chorowicz J, Yürür T, Froger JL, Köse O, Gündoğdu N (1998). Emplacement of volcanic vents and geodynamics of central Anatolia. *J Volcanol Geoth Res* 85: 33-54.
- Dirik K (2001). Neotectonic evolution of the northwestward arched segment of the Central Anatolian Fault Zone, Central Anatolia, Turkey. *Geodin Acta* 14: 147-158.



- Dirik K, Göncüoğlu MC, Kozlu H (1999). Stratigraphy and pre-Miocene tectonic evolution of the southwestern part of the Sivas basin central Anatolia, Turkey. *Geol J* 34: 303-319.
- Doğan U (2011). Climate-controlled river terrace formation in the Kızılırmak Valley, Cappadocia section, Turkey: inferred from Ar-Ar dating of Quaternary basalts and terraces stratigraphy. *Geomorphology* 126: 66-81.
- Ercan T (1986). Orta Anadolu'daki Senozoyik volkanizması. *MTA Dergisi* 107: 119-140 (in Turkish).
- Erkan Y (1981). An investigation about the metamorphism age of the Central Anatolian massif (Kırşehir region) by K-Ar methodology. *Yerbilimleri Dergisi* 8: 27-30.
- Frizon de Lamotte D, Raulin C, Mouchot N, Wrobel-Daveau JC, Blanpied C, Ringenbach JC (2011). The southernmost margin of the Tethys realm during the Mesozoic and Cenozoic: Initial geometry and timing of the inversion processes. *Tectonics* 30: TC3002.
- Froger JL, Lenat JF, Chorowicz J, Le Pennec JL, Bourdier JL, Köse O, Zimitoğlu O, Gündoğdu NM, Gourgaud A (1998). Hidden calderas evidenced by multisource geophysical data: example of Cappadocian calderas, Central Anatolia. *J Volcanol Geoth Res* 85: 99-128.
- Gautier P, Bozkurt E, Bosse V, Hallot E, Dirik K (2008). Coeval extensional shearing and lateral underflow during Late Cretaceous core complex development in the Niğde Massif, Central Anatolia, Turkey. *Tectonics* 27: TC1003.
- Gautier P, Bozkurt E, Hallot E, Dirik K (2002). Dating the exhumation of a metamorphic dome: geological evidence for pre-Eocene unroofing of the Niğde Massif (Central Anatolia, Turkey). *Geol Mag* 139: 559-576.
- Genç Y, Yürür T (2010). Coeval extension and compression in Late Mesozoic-Recent thin skinned extensional tectonics in central Anatolia, Turkey. *J Struct Geol* 32: 623-640.
- Güleç S (1996). Tuzköy (Nevşehir) ve civarındaki volkanitlerin mineralojisi ve petrografisi. MSc, Ankara University, Ankara, Turkey (in Turkish).
- Gülyüz E, Kaymakçı N, Meijers MJM, van Hinsbergen DJJ, Lefebvre C, Vissers R, Hendriks B, Peynircioğlu AA (2013). Late Eocene evolution of the Çiçekdağı Basin (Central Turkey): Syn-sedimentary compression during microcontinent-continent collision in Central Anatolia. *Tectonophysics* 602: 286-299.
- Gürsoy H, Piper JDA, Tatar O, Mesci L (1998). Palaeomagnetic study of the Karaman and Karapınar volcanic complexes, Central Turkey: neotectonic rotation in the South central sector of the Anatolian Block. *Tectonophysics* 299: 191-211.
- Hancock PL, Chalmers RML, Altunel E, Çakır Z (1999). Travertines: using travertines in active fault studies. *J Struct Geol* 21: 903-916.
- Hempton MR (1987). Constraints on Arabian plate motion and extensional history of the Red Sea. *Tectonics* 6: 687-705.
- İnan S (1993). Kızılırmak fay zonunun yapısal ve morfotektonik özellikleri. *Türk Jeol Kurumu Bül* 8: 321-328 (in Turkish).
- Innocenti F, Mazzuoli R, Pasquare G, Radicati di Brozolo F, Villari L (1975). The Neogene calc-alkaline volcanism of Central Anatolia: geochronological data on Kayseri-Niğde area. *Geol Mag* 112: 349-360.
- Kadioğlu YK, Dilek Y, Foland KA (2006). Slab break-off and syncollisional origin of the Late Cretaceous magmatism in the Central Anatolian Crystalline Complex, Turkey. *Geol S Am S* 409: 381-415.
- Karabacak V (2007). İhlara vadisi (Orta Anadolu) travertenlerinin genel özellikleri ve kabuksal deformasyon açısından önemleri. *Eskişehir Osmangazi Üniversitesi Mühendislik Mimarlık Fakültesi Dergisi* 20: 65-82 (in Turkish).
- Keller J (1974). Quaternary maar volcanism near Karapınar in Central Anatolia. *B Volcanol* 38: 378-396.
- Koçyiğit A (1976). Karaman-Ermenek (Konya) bölgesinde ofiyolitli melanj ve diğer oluşuklar. *Türk Jeol Kurumu Bül* 19: 103-115 (in Turkish).
- Koçyiğit A (1984). Intraplate neotectonic development in southwestern Turkey and its near environ. *Geol Soc Turkey Bull* 27: 1-16 (in Turkish with an abstract in English).
- Koçyiğit A (1991). An example of an accretionary forearc basin from northern Central Anatolia and its implications for the history of subduction of Neo-Tethys in Turkey. *Geol Soc Am Bull* 103: 22-36.
- Koçyiğit A (2003). Orta Anadolu'nun genel Neotektonik Özellikleri ve Depremselliği: Haymana-Tuzgölü-Ulukışla Basenleri Uygulamalı Çalışma. *TPJD Özel Sayı* 5: 1-26.
- Koçyiğit A (2005). Denizli Graben-Horst System and the eastern limit of the West Anatolian continental extension: basin fill, structure, deformational mode, throw amount and episodic evolutionary history, SW Turkey. *Geodin Acta* 18: 167-208.
- Koçyiğit A (2008). Orta Anadolu'nun aktif tektoniği ve jeotermal enerji potansiyeli. Ankara, Turkey: ODTÜ Jeoloji Mühendisliği Bölümü (in Turkish).
- Koçyiğit A (2009). Ankara'nın depremselliği ve 2005-2007 Afşar (Bala-Ankara) depremlerinin kaynağı. *Harita Dergisi* 141: 1-12 (in Turkish).
- Koçyiğit A, Beyhan A (1998). A new intracontinental transcurrent structure: the Central Anatolian Fault Zone, Turkey. *Tectonophysics* 284: 317-336.
- Koçyiğit A, Deveci Ş (2008). Ankara orogenic phase, its age and transition from thrusting-dominated palaeotectonic period to the strike-slip Neotectonic period, Ankara (Turkey). *Turkish J Earth Sci* 17: 433-459.
- Koçyiğit A, Erol O (2001). A tectonic escape structure: Erciyes pull-apart basin, Kayseri, Central Anatolia, Turkey. *Geodin Acta* 14: 133-145.
- Koçyiğit A, Türkmenoğlu A, Beyhan A, Kaymakçı N, Akyol E (1995). Post-collisional tectonics of Eskişehir-Ankara-Çankırı segments of İzmir-Ankara-Erzincan Suture zone: Ankara orogenic phase. *TABG Bull* 6: 69-86.

- Koçyiğit A, Yılmaz A, Adamia S, Kuloshvili S (2001). Neotectonic of East Anatolian Plateau (Turkey) and Lesser Caucasus: Implication for transition from thrusting to strike-slip faulting. *Geodin Acta* 14, 177-195.
- Köksal S, Gönçüoğlu C (1997). İdiş Dağı-Avanos Alanının Jeolojisi (Nevşehir, Orta Anadolu). *MTA Dergisi* 119: 73-87 (in Turkish).
- Kürçer A, Yeleser L, Karzaoğlu H, İzladı E, Aykaç S, Kutlu S, Köse K, Bostan S, Kurdal S (2012). Neotectonic Characteristics and Paleoseismology of Salt Lake Fault Zone, Central Anatolia, Turkey. MTA Report No. 11573. Ankara, Turkey: MTA.
- Le Pennec JL, Temel A, Froger JL, Şen S, Gourgaud A, Bourdier JL (2005). Stratigraphy and age of the Cappadocia ignimbrites, Turkey: reconciling field constraints with paleontologic, radiochronologic, geochemical and paleomagnetic data. *J Volcanol Geoth Res* 141: 45-64.
- McKenzie DP (1969). Speculations on the consequences and causes of plate motions. *Geophys J Roy Astr S* 30: 109-185.
- Mesci BL, Gürsoy H, Tatar O (2008). The evolution of travertine masses in the Sivas area (Central Turkey) and their relationships to active tectonics. *Turkish J Earth Sci* 17: 219-240.
- Metz K (1956). Aladağ ve Karanfil Dağı'nın yapısı ve bunların Kilikya Toros sistemiyle temsil edilen batı kenarları hakkında malumat husuli için yapılan jeolojik etüd. *MTA Dergisi* 48: 63-75 (in Turkish).
- Notsu K, Fujitani T, Ui T, Matsuda J, Ercan T (1995). Geochemical features of collision-related volcanic rocks in central and eastern Anatolia. *J Volcanol Geoth Res* 64: 171-192.
- Ocakoglu F (2004). Mio-Pliocene basin development in the eastern part of the Cappadocian Volcanic Province (Central Anatolia, Turkey) and its implications for regional tectonics. *Int J Earth Sci (Geologishe Rundschau)* 93: 314-328.
- Özsayın E, Çiner A, Rojaj B, Dirik K, Melnick D, Fernandez-Blanco D, Bertotti G, Schildgen TF, Garcin Y, Strecker MR et al. (2013). Plio-Quaternary extensional tectonics of the Central Anatolian Plateau: a case study from the Tuz Gölü Basin, Turkey. *Turkish J Earth Sci* 22: 691-714.
- Pasquare G (1968). Geology of the Cenozoic volcanic area of Central Anatolia. *Atti Acc Naz Lincei* 9: 53-204.
- Pasquare G, Poli S, Vezzoli L, Zanchi A (1988). Continental arc volcanism and tectonic setting in Central Anatolia, Turkey. *Tectonophysics* 146: 127-230.
- Platzman ES, Tapırdamaz C, Sanver M (1998). Neogene anticlockwise rotation of Central Anatolia (Turkey): preliminary palaeomagnetic and geochronological results. *Tectonophysics* 299: 175-189.
- Robertson AHF, Grasso M (1995). Overview of the Late Tertiary-recent tectonic and paleoenvironmental development of the Mediterranean region. *Terra Nova* 7: 114-127.
- Sassano G (1964). Acıgöl bölgesinde Neojen ve Kuvaterner volkanizması. MTA Rapor No: 6841. Ankara, Turkey: MTA (in Turkish).
- Şengör AMC, Yılmaz Y (1981). Tethyan evolution of Turkey: a plate tectonic approach. *Tectonophysics* 55: 361-376.
- Seymen I (1984). Geological evolution of the Kırşehir massif metamorphites. In: *Turkish Geological Society Ketin Symposium Proceedings*, pp. 133-148.
- Tan O, Tapırdamaz MC, Ergintav S, İnan S, İravul Y, Saatçılar R, Tüzel B, Tarancıoğlu A, Karakısa S, Kartal RF et al. (2010). Bala (Ankara) earthquakes: implications for shallow crustal deformation in Central Anatolian section of the Anatolian platelet (Turkey). *Turkish J Earth Sci* 19: 449-471.
- Tan O, Tapırdamaz MC, Yörük A (2008). The earthquake catalogues for Turkey. *Turkish J Earth Sci* 17: 405-418.
- Tatar O, Piper JDA, Gürsoy H (2000). Paleomagnetic study of the Erciyes sector of the Ecemiş fault zone: Neotectonic deformation in the south eastern part of the Anatolian Block. In: Bozkurt E, Winchester JA, Piper JDA, editors. *Tectonics and Magmatism in Turkey and the Surrounding Area*. London, UK: Geological Society Special Publications, pp. 423-440.
- Temiz U (2004). Kırşehir Dolayının Neotektoniği ve Depremselliği. PhD, Ankara University, Ankara, Turkey.
- Temiz U, Gökten E, Eikenberg J (2009). U/Th dating of fissure ridge travertines from the Kırşehir region (Central Anatolia Turkey): structural relations and implications for the Neotectonic development of the Anatolian block. *Geodin Acta* 22: 201-213.
- Tolluoğlu Ü (1993). Kırşehir Masifini kesen felsik intrüzyonların (Kötüdağ ve Buzlukdağ) petrografik ve jeokimyasal karakterleri. *Yerbilimleri Dergisi* 16: 19-41.
- Toprak V (1994). Central Kızılırmak Fault Zone: Northern margin of Central Anatolian Volcanics. *Turkish J Earth Sci* 3: 29-38.
- Toprak V (1996). Kapadokya volkanik çöküntüsünde gelişmiş Kuvaterner yaşlı havzaların kökeni, Orta Anadolu. In: *Karadeniz Teknik Üniversitesi Jeoloji Mühendisliği Bölümü 30. Yıl Sempozyumu*, Trabzon, Turkey, pp. 327-339.
- Toprak V (1998). Vent distribution and its relation to regional tectonics, Cappadocian Volcanics, Turkey. *J Volcanol Geoth Res* 85: 55-67.
- Toprak V, Gönçüoğlu MC (1993). Tectonic control on the development of Neogen Quaternary Central Anatolian volcanic province, Turkey. *Geol J* 28: 357-369.
- USGS (2016). United States Geological Survey, National Earthquake Information Center. Web page: <http://www.usgs.gov/>.
- Viereck-Goette L, Lepetit P, Gürel A, Ganskow G, Çopuroğlu İ, Abratis M (2010). Revised volcanostratigraphy of the Upper Miocene to Lower Pliocene Urgup Formation, Central Anatolian volcanic province, Turkey. *Geol S Am S* 464: 85-112.
- Whitney DL, Teyssier C, Dilek Y, Fayon AK (2001). Metamorphism of the Central Anatolian Crystalline Complex, Turkey: influence of orogen-normal collision vs. wrench dominated tectonics on P-T-t paths. *J Metamorph Geol* 19: 411-432.